



Assessment of groundwater sustainable development considering geo-environment stability and ecological environment: a case study in the Pearl River Delta, China

Peng Huang¹ · Chuanming Ma¹ · Aiguo Zhou¹

Received: 27 May 2021 / Accepted: 3 October 2021 / Published online: 22 October 2021
© The Author(s), under exclusive licence to Springer-Verlag GmbH Germany, part of Springer Nature 2021

Abstract

Groundwater resources have an important impact on the geo-environment and ecological environment. The exploitation of groundwater resources may induce geo-environmental issues and has a negative impact on the ecological environment. The assessment of groundwater sustainable development can provide reasonable suggestions for the management of groundwater resources in coastal cities. In this study, an assessment method for groundwater sustainable development based on the resource supply function, geo-environment stability function, and ecological environment function was provided. Considering the groundwater quantity and quality; the vulnerability of karst collapse, land subsidence, and seawater intrusion; and the distribution of groundwater-dependent ecosystems (GDEs) and soil erosion, the groundwater in the Pearl River Delta was divided into concentrated groundwater supply area (21.97%) and decentralized groundwater supply area (48.22%), ecological protection area (20.77%), vulnerable geo-environment area (8.94%), and unsuitable to exploit groundwater area (0.10%). ROC curve and single-indicator sensitivity analysis were applied in the assessment of geo-environment vulnerability, and the results showed that the VW-AHP model effectively adjusted the weights of the indicators so that the assessment results were more in line with the actual situation in the Pearl River Delta, and the accuracy of the VW-AHP model was higher than that of the AHP model. This study provides a scientific basis for groundwater management in the Pearl River Delta and an example for the assessment of groundwater sustainable development in coastal cities.

Keywords Groundwater sustainable development · Geo-environment vulnerability · Analytic hierarchy process · Variable weight theory · Pearl River Delta

Introduction

As an important part of the earth's water resources, groundwater plays an important role in the stability of the geo-environment and the balance of the ecosystem (Gholami et al. 2010). Groundwater is an important source of domestic, industrial, and agricultural water (Amiri et al. 2016; Bian et al. 2016; Panahi et al. 2017). However, the decline of the groundwater level caused by the unreasonable utilization of groundwater may lead to karst collapse, land subsidence,

and seawater intrusion (Bordbar et al. 2020; Fidelibus et al. 2011; Hakim et al. 2020a). Therefore, groundwater sustainable development is extremely important.

Groundwater is a natural resource that cannot be directly observed, so it is a challenging task to assess this resource (Allafta et al. 2021). Observation holes and stratum analysis are the most reliable and standard methods to identify the location of aquifers, groundwater quality, and hydraulic characteristics of aquifers, but they require a lot of time and manpower (Jha et al. 2010). Geophysical methods are important for determining the location of aquifers, groundwater recharge zones, and discharge zones, but they depend on physical nature distinctions and logistical support (Gugulothu et al. 2020). GIS is an effective tool for spatial analysis, display, and analysis of topographic data and integration with geographic data to solve well-defined problems by presenting geospatial data (Langat et al. 2020; Soyaslan 2020; Vahidnia et al. 2009). Simplified output can help

Responsible Editor: Xianliang Yi

✉ Chuanming Ma
machuanming@cug.edu.cn

¹ School of Environmental Studies, China
University of Geosciences, Wuhan 430074, Hubei,
People's Republic of China

decision-makers and other stakeholders make effective decisions (Slama and Sebei, 2020). Therefore, GIS technology can be used to assess groundwater sustainable development.

Multi-criteria decision analysis (MCDA) is considered an important tool for environmental decision-making to visualize and solve competitive decision-making issues (Asefi et al. 2020; Gupta et al. 2021; Janssen 1992; Sangrat et al. 2020; Steele et al. 2009). MCDA combines the advantages of qualitative standards and quantitative standards, so it has become the core of integrated solutions to solve issues (Tangestani 2004). The analytic hierarchy process (AHP) is the most appropriate MCDA technology to solve complex issues (Kumru and Kumru 2014; Vaidya and Kumar 2006). AHP is a theory that determines the relative importance of indicators through pairwise comparison and expert judgment, which can combine subjective and objective criteria (De Marinis and Sali 2020; Lee and Chan 2008). In this method, the complex issue is divided into several indicators. According to the relationship between the indicators, the indicators are combined to form a multilevel analysis structure model (Manca and Brambilla 2011; Wang et al. 2017). The analysis structure can be applied to explain the relationship between the system and the environment and the membership relation of the factors of the system (Hou et al. 2008). However, the application of AHP is limited because of a great number of assessment criteria, contradicting expert estimates, and incompatible matrices obtained (Podvezko 2009). The determination of the weight of the indicator is heavily affected by individual or group preferences, and decision-makers may find it difficult to make accurate judgments in many practical situations (Javanbarg et al. 2012; Yaraghi et al. 2015). To solve these issues, scholars have adopted a variety of methods to improve the AHP model, such as particle swarm optimization (Javanbarg et al. 2012), goal programming (Yu 2002), fuzzy technique (Turk and Ozkok 2020), and interval rough numbers (Pamucar et al. 2018). In addition, the weight of the indicator calculated by AHP is constant under different conditions. But in fact, the value of the indicator changes under different conditions, so AHP cannot express the weight of the indicator under different conditions (Chen et al. 2017). Changes in the value of indicators can lead to the “barrel effect,” which can play a decisive role in assessment after extreme deterioration (Zheng et al. 2020). The essence of variable weight theory is to introduce a state variable weight vector based on the constant weight of the indicator to ensure that the weight can be changed according to the value of the indicator or the diversified specific conditions (Yan et al. 2020). Therefore, the above problems can be effectively solved.

Groundwater sustainability is defined as a way to develop and use groundwater for an infinite time without causing environmental, economic, or social con-

sequences, which is time and space dependent (Alley et al. 1999; Pandey et al. 2011; Zhou et al. 2012). As the core issue of groundwater development, assessment and management of groundwater sustainability have received extensive attention (Chen, 2012). The essence of groundwater sustainability is to deal with the relationship between society, economy, environment, and groundwater resources, which implies the use of groundwater resources and future development in a sense to ensure the sustainable development of the environment and economy (Chen 2012; Singh and Bhakaru 2021). In this sense, groundwater sustainable development refers to the effective management of existing groundwater resources to meet current needs and to maintain storage capacity and recovery ability to meet future needs, which means that groundwater must be exploited and used efficiently and fairly to maintain its quality and environmental diversity (Das Gupta and Onta 1997; Raghavendra and Deka 2015). Currently, research on groundwater sustainable development focuses on identifying and predicting the potential of groundwater recharge (Adiat et al. 2012; Jhariya et al. 2016; Machiwal et al. 2015; Mandal et al. 2016; Sallwey et al. 2019; Singh et al. 2018) and establishment of indicator system and assessment method (Bui et al. 2019; Jia et al. 2019; Pandey et al. 2011).

The European Environment Agency (EEA) has introduced a driving force-pressure-state-impact-response (DPSIR) framework based on the principle that the pressure of social and economic development on the environment causes the environmental state to change (EEA 2003). An expert group convened by United Nations Educational, Scientific and Cultural Organization (UNESCO), International Atomic Energy Agency (IAEA), International Hydrological Programme (IHP), and International Association for Hydrogeology (IAH) put forward a report based on DPSIR and systematically introduced the goals and methods for the establishment of assessment indicators (Vrba and Lipponen 2007). Scholars around the world have carried out a lot of research on the assessment methods and indicators of groundwater sustainable development (Chen et al. 2015; Jothibasur and Anbazhagan 2018; Hosseini et al. 2019; Majidipour et al. 2021). As the most appropriate MCDA technology, AHP has been applied in the assessment of groundwater sustainable development at community scale (Sullivan 2002), urban scale (De Carvalho et al. 2009), watershed scale (Kang and Lee 2011), and national scale (Jia et al. 2019). Al-Zu’bi et al. (2002) proposed an AHP-based decision support system whose input was generated by Modflow (groundwater), stochastic, Penman Montieth models, and water productivity for agricultural and industrial sectors, and made recommendations for the long-term

sustainability of water resources in the Azraq Basin in Jordan. Karamouz et al. (2018) calculated the planning for sustainable use index based on AHP and assessed the impact of the artificial groundwater recharge on the groundwater sustainable development in the Gorveh-Dehgolan Plain. Aslan and Celik (2021) considered ten indicators whose weights were determined by AHP and calculated the groundwater potential index of the Harran Basin in Turkey. Dilekoglu and Aslan (2021) used the weighted overlay analysis method and the fuzzy analytical hierarchy process to identify the groundwater potential area of the Ceylanpinar Plain in Upper Mesopotamia. Even if the research on AHP of various spatial scales and its improvement methods is sufficient, the quality and reliability of the indicators still need to be evaluated by appropriate standards (Pires et al. 2017). Therefore, it is necessary to introduce a concept to clarify the relationship between an indicator and its comprehensive index (Bui et al. 2018).

At present, there is a lack of work related to the assessment of groundwater sustainable development on a global scale as well as a comprehensive analysis of quantitative composite indicators (Hosseini et al. 2019). Therefore, more research on assessment methods is needed. The amount of groundwater recharge is the total number of renewable resources. To avoid groundwater depletion and geological and ecological problems caused by the decline of groundwater level, groundwater extraction should be less than groundwater recharge (Guo et al. 2019; Paz et al. 2020). Therefore, indicators can be selected from three functions of groundwater to assess the sustainable development of groundwater (CGS 2006).

Function 1. Resource supply function emphasizes the potential of groundwater development, including groundwater quantity and quality.

Function 2. Geo-environment stability function is used to identify geo-environmental issues arising from groundwater development.

Function 3. Ecological environment function is used to assess the impact of groundwater development on the ecosystem.

Water resources are abundant in the Pearl River Delta. With the development of the economy, water consumption has continued to increase, and surface water pollution has become increasingly serious (Wang and Jiao 2012; Zhang et al. 2015, 2019a; Jia et al. 2018). Therefore, groundwater has become an important source of water supply. Groundwater resources in the Pearl River Delta region are unevenly distributed (IHEG 2010). Unreasonable exploitation of groundwater leads to karst collapse, land subsidence, and seawater intrusion (Gao et al. 2019). In the last two decades, seawater intrusion has gradually become severe,

which severely affected the freshwater resources (Huang et al. 2004; Liu et al. 2018). Reduced quantity and increased pollution of groundwater also have adverse effects on the ecosystem (Liu et al. 2018). In response to these problems, China has adopted some effective groundwater management measures, such as the promulgation of the Water Law of the People's Republic of China and the Guidelines for the assessment of zones of groundwater overdraft (GB/T 34,968–2017) (MLR 2017a). However, these measures are remedial and cannot fundamentally prevent overexploitation of groundwater. Therefore, assessing the groundwater sustainable development and delimiting the supply areas and protection areas of groundwater are effective measures to realize the management of groundwater resources. In this study, taking the Pearl River Delta as the study area, the groundwater sustainable development is assessed in combination with the resource supply function, geo-environment stability function, and ecological environment function. For example, the groundwater supply areas are determined based on groundwater quality and quantity. A model that combines AHP and variable weight theory (VW-AHP model) is used to determine the vulnerable geo-environment areas. The distribution areas of the groundwater-dependent ecosystems and the distribution areas of soil erosion are identified as ecological as ecological protection areas. The main purpose of this study is to provide a plan for groundwater sustainable development in the Pearl River Delta and groundwater management in coastal cities.

Study area

The Pearl River Delta is located in the south-central part of Guangdong Province, adjacent to the South China Sea to the south, across 112°0'E–115°24'E longitude and 21°43'N–23°56'N latitude, covering an area of 41,698 km² (Fig. 1d). The altitude of the study area is low in the middle and high in the west, north, and east (Fig. 1c). The alluvial plain is the main landform of the study area, and low mountains, hills, and tablelands are distributed in the west, north, and east of the study area (Hou et al. 2018; Liu et al. 2017). The surface water system is widely distributed, such as the Xijiang River and the Dongjiang River, which originated in mountains and were merged into the South China Sea (Wei and Wu 2011). The climate in the study area is warm and humid, and the annual average temperature is 14–22°C (Wu et al. 2016). Affected by the monsoon, rainfall varies greatly in time and space, concentrated in summer (Huang et al. 2018). The average annual precipitation is 1600 mm, which can reach 2000–2600 mm in some mountainous areas (Fig. 1b).

Groundwater in the study area mainly occurs in loose sediment pores, carbonate rock fractures, and bedrock fractures.

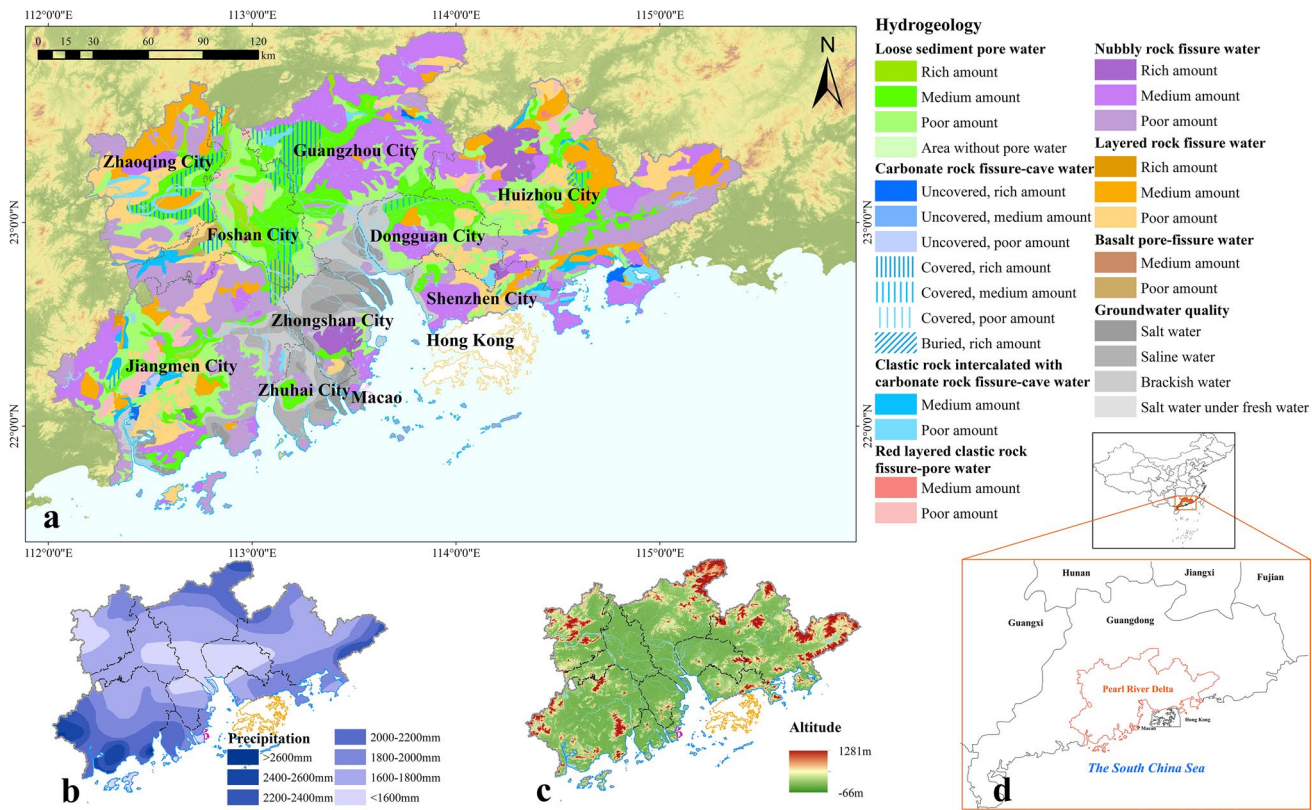


Fig. 1 Location, altitude, precipitation, and hydrogeology of the study area: **a** hydrogeology, **b** precipitation, **c** altitude, and **d** location

The loose sediment pore water is distributed in alluvial plains, and the lithology of the aquifer is mainly medium-coarse sand and gravel, with medium or rich water (Fig. 1a) (CGS 1979, 1981). The water quality in hilly areas and mountainous areas in the northwest of the study area is relatively good, and the water quality near the coastal and the Pearl River estuary is poor due to seawater intrusion and pollution from human activities (Li et al. 2020b; Liu et al. 2014; IHEG 2010; Wang et al. 2016; Zhang et al. 2020). The main recharge source of loose sediment pore water is the surface overflow formed by atmospheric precipitation, which infiltrates directly through the sand layer and discharges to nearby rivers (Zhang et al. 2019a). The hydraulic relationship between groundwater and surface water is complex (Zhang et al. 2005).

The uncovered carbonate rock fissure-cave water is scattered, and the lithology of the aquifer is mainly limestone, dolomite, marble, and argillaceous limestone, with poor or medium water (Fig. 1a) (CGS 1979, 1981). The covered carbonate rock fissure-cave water is mainly distributed in the northwest of the study area. The lithology of the aquifer is mainly limestone, marble, and argillaceous limestone, with well-developed fissures (CGS 1979, 1981). The water quantity is medium or rich, and the water quality is generally good (Fig. 1a) (IHEG 2010).

The main sources of groundwater recharge include atmospheric precipitation infiltration, river infiltration, and irrigation infiltration. In low mountainous areas and hilly areas, groundwater is mostly discharged to neighboring valleys or in the form of springs (Zhang and Li 2005). The fissure water flows into the plain areas through the hilly areas, part of which replenishes the pore water, and the other part becomes an underground undercurrent (IHEG 2010). The groundwater in plain areas generally flows from north to south and finally discharges into the South China Sea through the Pearl River and Lingdingyang Sea (GHST 1981; Wang et al. 2016). The main influencing indicator of the changes in groundwater level and reserves is precipitation, followed by irrigation infiltration, showing seasonal changes.

The decline of groundwater level due to unreasonable exploitation of groundwater is the main reason for seawater intrusion in the study area (Wu et al. 2020). Affected by seawater intrusion, brackish water, saline water, and salty water distinguished by total dissolved solids (TDS) are widely distributed in coastal plains near the Pearl River estuary (Wu et al. 2020). As a result of large-scale exploitation of groundwater, a large number of karst collapses occurred around the groundwater source area (Dong et al. 2012). Large-scale drainage in engineering construction is also an important cause of karst collapse (WCGS 2015). At present, more

than 100 karst collapses have occurred in the study area. Overexploitation of groundwater is the main cause of land subsidence (Zhang and Li 2005). Besides, the compression of aquifers caused by large-scale high-rise building construction and underground space development are also inducing indicators for land subsidence (WCGS 2015).

Methods

Technical route

In this study, the functions of groundwater are summarized as resource supply function, geo-environment stability function, and ecological function. Geo-environment stability function is assessed using the VW-AHP model, which is combined with groundwater quantity, quality, and ecological environment to assess the groundwater sustainable development (Fig. 2).

Analytic hierarchy process

AHP was proposed by Saaty (1980) with a simple principle and reliable theoretical basis. A large number of practical cases prove that AHP has strong practicality in solving complex multi-objective competitive decision-making

problems (Bao et al. 2016; Besikci et al. 2016; Nouri et al. 2018; Peng and Peng 2018; Yadegaridehkordi et al. 2018; Zarghami et al. 2018; Zhang et al. 2021). AHP usually consists of three steps.

Step 1. Construction of the hierarchical structure. The hierarchical structure is to explain the system of interactions between the various components within a complex issue (Unver and Ergenc 2021). The determination of indicators mainly relies on the knowledge and experience of decision-makers and relevant experts.

Step 2. Pairwise comparison of indicators. According to the judgment of decision-makers or experts, the relative importance of indicators is determined through the pairwise comparison. A scale from 1 to 9, including odd numbers, even numbers only as a compromise value, is used in the pairwise comparison (Reddy et al. 2014). The judgment matrix *A* obtained by pairwise comparison is used to calculate the weight of each indicator. The judgment matrix *A* is calculated by Eq. 1. The dimension *n* of the matrix is the number of indicators.

$$A = \begin{bmatrix} a_{11} & \cdots & a_{1n} \\ \vdots & \ddots & \vdots \\ a_{n1} & \cdots & a_{nn} \end{bmatrix} \tag{1}$$

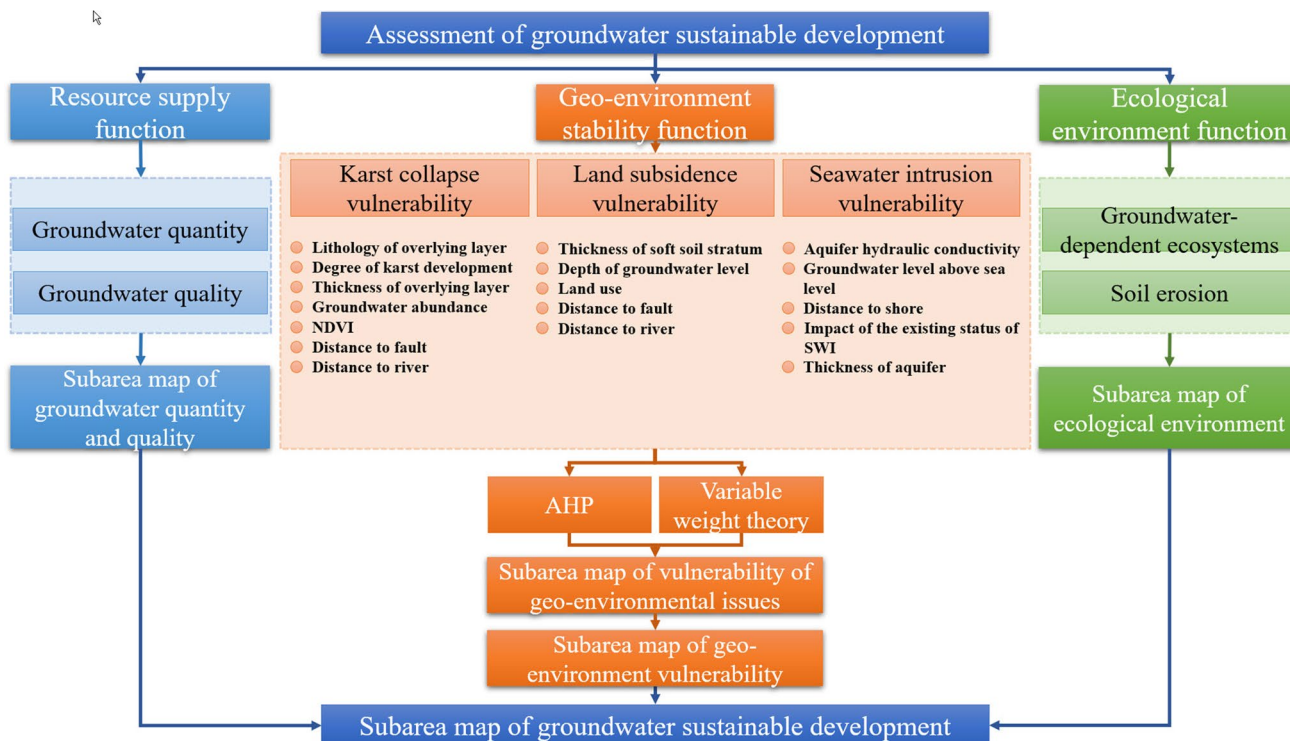


Fig. 2 Flowchart of this study

To prevent the element values in judgment matrix A from varying too much, the elements in the matrix are normalized. The calculation method of the elements in the normalized matrix is shown in Eq. 2.

$$b_{ij} = \frac{a_{ij}}{\sum_{i=1}^n a_{ij}} \tag{2}$$

To calculate the eigenvector that matches the maximum eigenvalue, Eq. 3 is used to calculate the average value of the row elements of the normalized matrix.

$$w_i = \frac{\sum_{j=1}^n b_{ij}}{n} \tag{3}$$

The calculation of the maximum eigenvalue value can be found in Eq. 4.

$$\lambda_{\max} = \frac{1}{n} \sum_{i=1}^n \frac{(Aw)_i}{w_i} \tag{4}$$

Step 3. Check of consistency ratio. Whether a decision-maker can make the right decision is determined by the consistency of the pairwise comparison. The higher the consistency is, the more accurate the result of the pairwise comparison is. If the consistency is low, the pairwise comparison of the indicators needs to be repeated. The calculation method of the consistency index (CI) used to accept the consistency ratio of the judgment matrix can be found in Eq. 5.

$$CI = \frac{\lambda_{\max} - n}{n - 1} \tag{5}$$

The calculation method of consistency ratio (CR) used to eliminate inconsistency is shown in Eq. 6.

$$CR = \frac{CI}{RI} \tag{6}$$

In Eq. 6, RI is the average random consistency index. When the CR is less than or equal to 0.10, insistency is acceptable.

Variable weight theory

In the AHP method, the weight of the indicator is constant. However, when the value of some indicators is extremely large or extremely small, the value of these indicators will have a significant impact on the assessment results. Therefore, in this study, the variable weight theory is introduced. The weight of the indicator is adjusted according to the value of the indicator so that the assessment result can better reflect the actual situation. The variable weight theory was proposed by Wang (1985) and has been widely used in many fields (Liu and Li

2019; Wang et al. 2020; Wu et al. 2017; Zhang et al. 2019b). The connection between the weight vector and the state vector is established by a variable weight function, so the weight of the indicator can be adjusted as the decision state changes (Lin et al. 2020). According to the monotonicity of the variable weight function, there are three types of variable weight functions: penalty type, incentive type, and penalty-incentive type (Shu et al. 2017). In this study, the value of the indicator is negatively related to the vulnerability of geo-environmental issues. Therefore, the penalty type variable weight formula is used to modify the constant weight.

The state variable weight vector is defined by Eq. 7.

$$s_i = (x_i)^{\alpha-1} \tag{7}$$

The calculation method of the variable weight vector is shown in Eq. 8.

$$w'_i = \frac{w_i s_i}{\sum_{i=1}^n w_i s_i} \tag{8}$$

In Eqs. 7 and 8, x_i is the value of indicator i . s_i is the state variable weight vector of indicator i . w_i is the constant weight vector of indicator i . w'_i is the variable weight vector of indicator i . α is the equilibrium coefficient between 0 and 1. In this study, α is assigned a value of 0.2.

Finally, a comprehensive index (CPI) of the vulnerability of geo-environmental issues is given by Eq. 9.

$$CPI = \sum_{i=1}^n w'_i x_i \tag{9}$$

Analyses and results

Resource supply function

Groundwater quantity

In this study, the assessment of exploitable groundwater resources is the main content of groundwater quantity. According to the principle of water balance, the number of exploitable groundwater resources is related to groundwater recharge, which can be quantitatively described by the modulus of groundwater exploitability (MGE) (Ding 2018; MWR 2005; Ma 2018). MGE is the number of groundwater resources allowed to be exploited per unit area, as shown in Eq. 10.

$$MGE = \frac{TR \times \rho}{F} \tag{10}$$

In Eq. 10, TR is the total recharge of a single hydrogeological unit. ρ is the extraction coefficient. F is the area of a single hydrogeological unit.

The divisions of MGE are based on administrative districts (Table 1). The MGE is higher in low mountainous

areas and hilly areas. Among them, the MGE is the highest in northern Huizhou, northern Guangzhou, northern Zhaoqing, and western Jiangmen, which is greater than $40 \times 10^4 \text{ m}^3/(\text{a} \cdot \text{km}^2)$. The MGE of alluvial plains is low, among which the MGE of southern Guangzhou and northern Zhuhai is the lowest, less than $10 \times 10^4 \text{ m}^3/(\text{a} \cdot \text{km}^2)$. The data of groundwater quantity in the study area is provided by Wuhan Center of Geological Survey, as shown in Fig. 3a.

Groundwater quality

A total of 1906 groups of samples of groundwater quality were obtained from 1467 wells and 32 springs in the study area and tested according to the requirements of MLR (2017b). There are 3 on-site indicators, 34 inorganic indicators, and 61 organic indicators used for groundwater quality analysis.

Each indicator is classified into five classes, from class I to class V (MLR 2017b). The class of groundwater quality

is determined based on the class of each indicator according to the “barrel effect,” that is, the class of groundwater quality is determined by the worst among the classes of indicators. Class I means the best quality, while class V means the opposite. The groundwater of classes I–III can be used as a source of drinking water. The groundwater of class IV can be used as a source of industrial and agricultural water and can be used as a source of drinking water after proper treatment. The groundwater of class V is not suitable as a source of drinking water.

The groundwater quality in the study area is generally good. The main classes of groundwater are class I–III. The groundwater of class IV and class V is mainly distributed in urban land, farmland, and garden. The data of groundwater quality in the study area is provided by Wuhan Center of Geological Survey, as shown in Fig. 3b.

Geo-environment stability function

Assessment indicator

Karst collapses usually develop from soil holes in limestone-covered areas, under the effect of groundwater (De Waele et al. 2011; Drobinina et al. 2020; Jiang et al. 2019). In China, karst collapse has developed very rapidly in recent years, posing a serious threat to the natural environment and social economy (Zhao et al. 2018). In the study area, the general scale of karst collapse is small, but a large number of them occurred in urban land, so they are more harmful. The occurrence of karst collapse is caused by many indicators. Based on previous research and the situation in the study area, seven indicators were selected as assessment indicators of karst collapse vulnerability (Calligaris et al. 2017; He et al. 2013; Ozdemir, 2016; Salles et al. 2018; Taheri et al. 2015, 2019; Wei et al. 2021; Wu et al. 2018; Yilmaz 2007).

Lithology of overlying layer (L) The lithology of overlying layer is the material basis for the occurrence of karst collapse. In areas covered by limestone and dolomite, karst collapse is more likely to occur because these two types of rocks are more soluble. Compared with limestone and dolomite, sandstone, sandy conglomerate, tuff, and argillaceous limestone are slightly less soluble. Claystone, mudstone, shale, and argillaceous sandstone have worse solubility. There is almost no karst developed in other lithology of overlying layer. Therefore, the lithology of overlying layer is classified into four ranges. Lithology data is provided by Wuhan Center of Geological Survey.

Degree of karst development (D) The degree of karst development reflects the characteristics of the number, scale, and connectivity of the cracks and cavities produced by the dissolution of groundwater in the soluble rock. The stronger

Table 1 Modulus of groundwater exploitability of each unit

Unit	TR ($10^4 \text{ m}^3/\text{a}$)	ρ	F (km^2)	MGE ($10^4 \text{ m}^3/(\text{a} \cdot \text{km}^2)$)
Sihui	70,275	0.75	1308.31	40.29
Gaoyao	97,203	0.65	2264.75	27.90
Dinghu	29,823	0.75	731.50	30.58
Sanshui	27,296	0.69	856.63	21.99
Gaoming	37,680	0.69	868.16	29.95
Heshan	39,664	0.85	1120.75	30.08
Kaiping	81,941	0.69	1716.59	32.94
Enping	88,555	0.88	1752.98	44.45
Taishan	137,824	0.75	2971.27	34.79
Doumen	9310	0.69	858.81	7.48
Zhuhai	21,858	0.85	693.67	26.78
Xinhui	36,114	0.85	1731.02	17.73
Jiangmen	2319	0.85	114.13	17.27
Zhongshan	30,620	0.90	1808.55	15.24
Shunde	17,306	0.85	834.08	17.64
Nanhai	27,764	0.85	1187.52	19.87
Foshan	1933	0.85	80.42	20.43
Guangzhou	51,376	0.90	1522.20	30.38
Panyu	7709	0.85	659.65	9.93
Huadu	31,431	0.90	1001.67	28.24
Zengcheng	75,099	0.88	1667.31	39.64
Conghua	93,573	0.88	2051.14	40.15
Boluo	157,863	0.88	3024.18	45.94
Huizhou	15,235	0.69	402.30	26.13
Dongguan	51,019	0.90	2531.27	18.14
Shenzhen	69,593	0.90	2060.11	30.40
Huiyang	80,729	0.85	2263.43	30.32
Huidong	167,394	0.65	3615.61	30.09

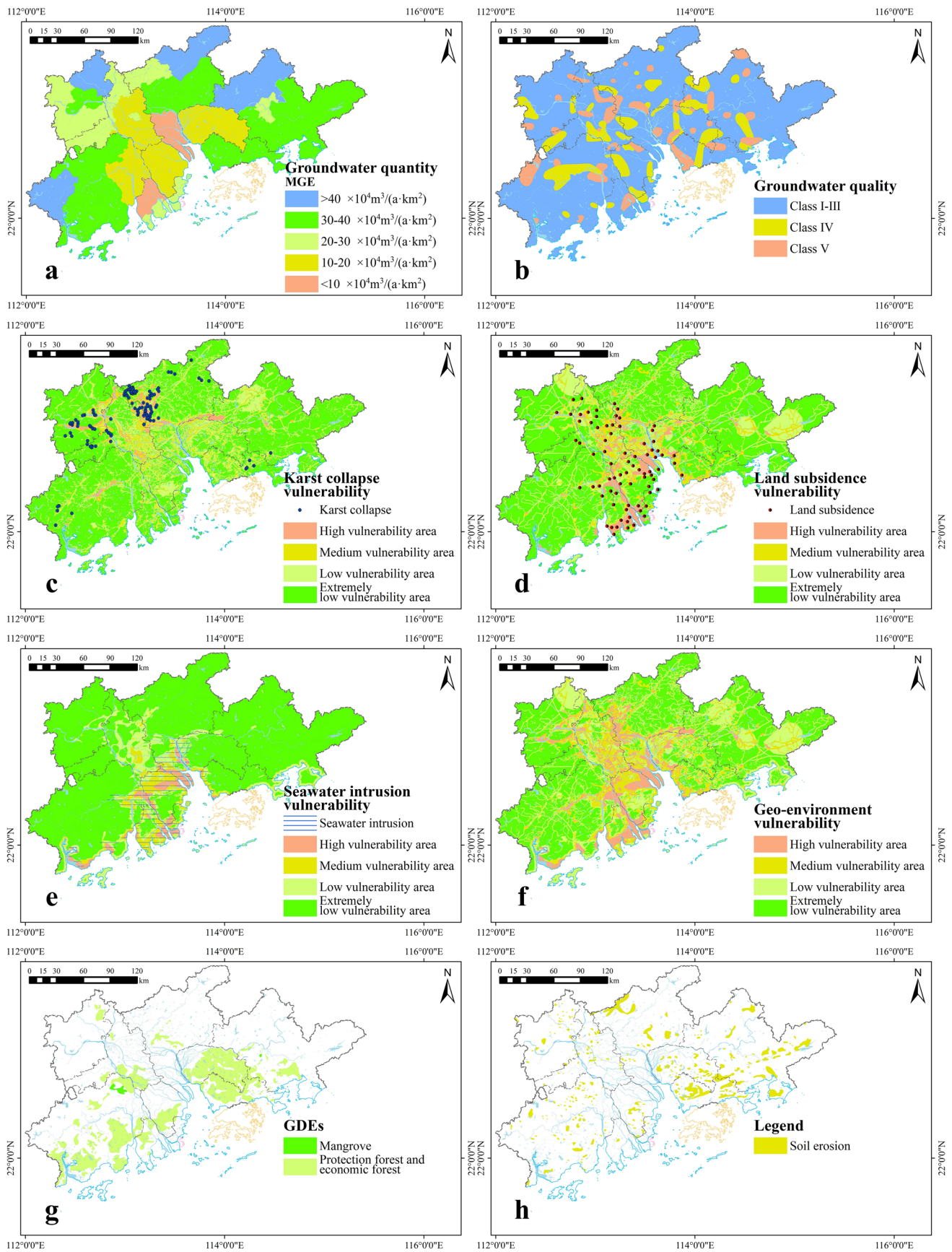


Fig. 3 Distribution maps of the indicators of the assessment of groundwater sustainable development: **a** groundwater quantity, **b** groundwater quality, **c** karst collapse vulnerability, **d** land subsidence vulnerability, **e** seawater intrusion vulnerability, **f** geo-environment vulnerability, **g** GDEs, **h** soil erosion

the degree of karst development is, the greater the tendency for karst collapse to occur is. In this study, the degree of karst development is classified into four ranges: very strong, strong, not strong, and no karst. The data of the degree of karst development is provided by Wuhan Center of Geological Survey.

Thickness of overlying layer (T) The thickness of overlying layer has an impact on the occurrence of karst collapse. Karst collapse mostly occurs in areas where the overlying layer is thin or has joints. The structural strength of the overlying layer in these areas is low, and karst collapse is prone to occur. The thickness of overlying layer is classified into four ranges: < 5 m, 5–10 m, 10–20 m, and > 20 m. Data of the thickness of overlying layer is provided by Wuhan Center of Geological Survey.

Groundwater abundance (G) Groundwater is the dynamic condition for karst development. Groundwater flows in soluble rock fissures and cavities and continuously dissolves the soluble rock, which is a favorable condition for the development and expansion of soil cavities. The outflow rate of single well is used to describe the groundwater abundance. Larger outflow rate of single well means greater groundwater abundance. The outflow rate of single well is classified into three ranges: 0–100 m³/day, 100–1000 m³/day, and > 1000 m³/day. The data was provided by Wuhan Center of Geological Survey.

NDVI (M) Normalized vegetation difference index (NDVI) is an indicator used to describe the activities of vegetation, effectively reflecting the growth state of vegetation (Amano and Iwasaki 2020; Chen et al. 2020; Cunliffe et al. 2020; Almouctar et al. 2021). Refer to Eq. 11 for the calculation method of NDVI.

$$\text{NDVI} = \frac{\text{NIR} - \text{Red}}{\text{NIR} + \text{Red}} \quad (11)$$

In Eq. 11, NIR represents the spectral characteristics of the near-infrared band and Red represents the spectral characteristics of the red light band. Using ArcGIS 10.6, NDVI in the study area is calculated from the spectral reflectance measurements and is classified using natural break classification (Kumar and Anbalagan, 2015), which is classified into four ranges: < 0.2727, 0.2727–0.4764, 0.4764–0.6709, and > 0.6709. The spectral reflectance measurements are

extracted on the remote sensing images which are provided by China Geological Survey.

Distance to fault (F) In the fault zone, the broken rock structure leads to a large number of fissures. The developed and interconnected fissures become a good channel for groundwater flow, and the flowing groundwater has a strong dissolution ability. Under better fracture conditions, soluble rock can get full contact with groundwater, and it also contributes to the dissolution of soluble rock. In this study, the distance to fault is considered the assessment indicator. In ArcGIS 10.6, the Euclidean distance method (He et al. 2012) is used to classify the distance to fault into four ranges: < 500 m, 500–1000 m, 1000–1500 m, and > 1500 m. The fault is extracted on the geological map of the study area provided by Wuhan Center of Geological Survey.

Distance to river (R) The river has an impact on the occurrence of karst collapse. The groundwater circulation between river water and groundwater enhances the mobility of groundwater and increases the possibility of dissolution of soluble rock. The replenishment of groundwater by river water increases groundwater abundance. The distance to river can be used as an assessment indicator. In ArcGIS 10.6, using the Euclidean distance method, the distance to river is classified into four ranges: < 300 m, 300–600 m, 600–900 m, and > 900 m. The river data is extracted on the remote sensing images.

Land subsidence refers to the phenomenon of unexpected rapid or slow subsidence that occurs when there is almost no horizontal movement of the ground (USGS 2020). Large-scale exploitation of groundwater is the main cause of land subsidence. The compression of aquifer caused by engineering activities such as the construction of high-rise buildings in distribution areas of soft soil stratum may also cause land subsidence. The occurrence of land subsidence is affected by geological conditions and human activities. Based on this, five indicators were selected as assessment indicators of land subsidence vulnerability (Arabameri et al. 2020; Ebrahimi et al. 2020; Fadhillah et al. 2020; Hakim et al. 2020b; Jia et al. 2017; Mohammady et al. 2019; Najafi et al. 2020; Oh et al. 2019; Rahmati et al. 2019; Tafreshi et al. 2020).

Thickness of soft soil stratum (T) The existence of soft soil stratum is a prerequisite for land subsidence. Affected by the additional stress, the soft stratum will consolidate and cause land subsidence. The thickness of soft soil stratum provided by Wuhan Center of Geological Survey is classified into four ranges: > 20 m, 10–20 m, < 10 m, and no soft soil stratum.

Depth of groundwater level (D) Excessive exploitation of groundwater is one of the causes of land subsidence. Since reliable data of groundwater drawdown cannot be obtained,

the depth of groundwater level is used to reflect the state of groundwater extraction. The greater the depth of groundwater level is, the greater the tendency for land subsidence to occur is. There are 113 observation holes in the study area, and the groundwater level is directly obtained from the observation data. Combined with the elevation of the observation hole, the depth of groundwater level can be obtained. In ArcGIS 10.6, the observed data of depth of groundwater level is interpolated by inverse distance weighted interpolation (Mueller et al. 2001) to obtain the distribution of depth of groundwater level in the study area. The interpolated data is classified into four ranges by natural break classification: > 3.03 m, 2.10–3.03 m, 1.32–2.10 m, and < 1.32 m. The locations and groundwater levels of the 113 observation holes were provided by Wuhan Center of Geological Survey.

Land use (L) Groundwater is an important source of water for domestic and agricultural water. Besides, construction activities in urban land will increase the ground load. Both of these causes will induce land subsidence. Land use is classified into three ranges: urban land, agricultural land, and the others in this study. The data of land use is provided by Wuhan Center of Geological Survey.

Distance to fault (F) The strength and permeability of rocks and soil are affected by the structure, so the occurrence of land subsidence is related to the structure. Land subsidence is more likely to occur in the fault zone because the fault zone is structurally active. In ArcGIS 10.6, the Euclidean distance method is used to classify the distance to fault into four ranges: < 500 m, 500–1000 m, 1000–1500 m, and > 1500 m.

Distance to river (R) There is a hydraulic connection between river water and groundwater, which affects the groundwater level. Therefore, the distance to river indirectly affects the occurrence of land subsidence. In ArcGIS 10.6, the distance to river is classified into four ranges: < 300 m, 300–600 m, 600–900 m, and > 900 m using the Euclidean distance method.

Seawater intrusion is a global problem caused by excessive pumping of aquifers, land use changes, and climate change (Rachid et al. 2021). The GALDIT method is an overlay and indicator technique that considers a variety of indicators that may directly or indirectly affect the hydrodynamic process leading to seawater intrusion and is used to assess the seawater intrusion vulnerability of coastal aquifers (Bordbar et al. 2019; Chang et al. 2019; Seenipandi et al. 2019). The method is based on hydrogeological features (depth of the water body, thickness of the aquifer), morphology (distance to coast), hydrodynamics (transmissivity), and chemical properties (impact of marine intrusion) (Hallal et al. 2019). The GALDIT method is used to assess

the seawater intrusion vulnerability through indicator classification, weight determination, and linear weighting. In this method, six indicators are selected, including groundwater occurrence (*G*), aquifer hydraulic conductivity (*A*), groundwater level above sea level (*L*), distance to shore (*D*), impact of the existing status of seawater intrusion (*I*), and thickness of aquifer (*T*) (Kazakis et al. 2018; Luoma et al. 2017; Mahrez et al. 2018; Moghaddam et al. 2017; Recinos et al. 2015). Considering that the assessment object is a shallow aquifer, groundwater occurrence is not used as an assessment indicator (Guo et al. 2019).

Aquifer hydraulic conductivity (A) Hydraulic conductivity reflects the ability of the aquifer to transport water and controls the flow rate of groundwater. In the case of the same hydraulic gradient, the greater the aquifer hydraulic conductivity is the greater the groundwater depression cone generated during the pumping process is, and the greater the possibility of the occurrence of seawater intrusion is. The horizontal value of hydraulic conductivity is determined according to the lithology of the aquifer provided by Wuhan Center of Geological Survey (CGS 2012). The hydraulic conductivity of coarse sand, gravel, and bedrock is > 25 m/day and that of medium sand is 10–25 m/day. The hydraulic conductivity of silty sand and fine sand is 1–10 m/day, while that of clay and loess is < 1 m/day.

Groundwater level above sea level (L) Whether the seawater and groundwater in freshwater aquifers can maintain a dynamic balance is determined by the groundwater level. The possibility of seawater intrusion increases when the groundwater level of the freshwater aquifer is lower than the seawater level. In this study, groundwater level above sea level is classified into four ranges: < -2 m, 0–2 m, 0–2 m, and > 2 m. The relevant data of groundwater level is provided by Wuhan Center of Geological Survey.

Distance to shore (D) The influence of tidal movement decreases as the distance of movement increases. Therefore, the possibility of aquifers being affected by seawater intrusion decreases as the distance to shore increases. In ArcGIS 10.6, the Euclidean distance method is used to calculate the distance to shore based on the shore data extracted on the remote sensing images. The distance to shore is classified into four ranges: < 2.5 km, 2.5–5 km, 5–10 km, and > 10 km.

Impact of the existing status of seawater intrusion (I) Due to the seawater intrusion caused by the continuous exploitation of groundwater in the study area, the saltwater/freshwater interface has moved to the freshwater aquifer. In this study, TDS is used to describe the distribution of the existing status of seawater intrusion, which can be classified into four

ranges: > 10 g/L, 3–10 g/L, 1–3 g/L, and < 1 g/L. TDS data is provided by Wuhan Center of Geological Survey.

Thickness of aquifer (T) The degree to which the saturation zone is affected by seawater intrusion is positively correlated with the thickness of aquifer. The thickness of aquifer provided by Wuhan Center of Geological Survey is classified into four ranges: > 30 m, 20–30 m, 10–20 m, and < 10 m.

Each indicator is assigned a rating of 0.1, 0.4, 0.7, and 1.0 according to four ranges. If the indicator is classified into only three ranges, it is given a rating of 0.1, 0.55, and 1.0 (Daneshvar 2014; Das 2018; Narimani et al. 2021; Quan et al. 2012; Veerappan et al. 2017).

Constant weight determination

The AHP method is used to calculate the constant weight of each indicator, including three steps: the construction of the judgment matrix, the calculation of the constant weight, and the consistency check.

Variable weight determination

Low ratings of indicators indicate high vulnerability to geo-environmental issues. Therefore, the penalty-type variable weight formula is used to calculate the variable weight. State variable weight vector and variable weight vector are calculated using Eqs. 7 and 8. For each indicator, the constant weight is constant, and the variable weight changes according to the rating of the indicator.

Assessment unit division

The irregular polygon mesh method (Sun et al. 2019) is used to divide the assessment unit. Specifically, the distribution map of each indicator is superimposed in ArcGIS 10.6 to become a subarea map of the vulnerability of geo-environmental issues. Each closed polygon is regarded as an assessment unit. In an assessment unit, the rating of an indicator is uniform, which avoids the error caused by uneven rating. In the vulnerability assessment of karst collapse, land subsidence, and seawater intrusion, the study area is divided into 192,014, 34,993, and 22,068 assessment units, respectively (Fig. 4a, b, and c).

Comprehensive index determination

The CPI of each assessment unit is calculated using Eq. 9. For each assessment unit, CPI is equal to the sum of the product of the rating of each indicator and the corresponding variable weight vector.

Vulnerability assessment of geo-environmental issues

The CPI of the vulnerability assessment of geo-environmental issues is classified by natural break classification. According to the results of the classification, the extremely low vulnerability area, low vulnerability area, medium vulnerability area, and high vulnerability area are determined (Fig. 3c, d, and e and Table 2) (Achour et al. 2017; Domazetovic et al. 2019; Javidan et al. 2021; Myronidis et al. 2016).

Geo-environment vulnerability assessment

Due to the “barrel effect,” as long as there is a high-vulnerability area of a geo-environmental issue, the subarea is assessed as a high-vulnerability area of geo-environment. Only when a subarea is an extremely low-vulnerability area of all geo-environmental issues, the subarea can be assessed as an extremely low-vulnerability area of the geo-environment. In other words, the vulnerability level of the geo-environment is determined by the highest vulnerability level of geo-environmental issues in an assessment unit. According to these principles, the extremely low-vulnerability area, low-vulnerability area, medium-vulnerability area, and high-vulnerability area are divided (Fig. 3f and Table 2). The study area is divided into 394,118 assessment units (Fig. 4d).

The high-vulnerability areas of the geo-environment are mainly distributed in delta plains, river terraces, marine plains, and coastal areas of Jiangmen and Zhuhai. The high-vulnerability areas of karst collapse are not only mainly distributed in the Zhaoqing-Foshan-Guangzhou-Huizhou area but also scattered in parts of Jiangmen and Huizhou. The lithology of overlying layer is dominated by carbonate rock, sandstone, and sandy conglomerate, most of which are less than 5 m. The high-vulnerability areas of land subsidence are mainly distributed in the Guangzhou-Zhongshan-Jiangmen-Zhuhai area and sporadically distributed along faults in other areas. The thickness of soft soil stratum in these areas is more than 20 m. The depth of groundwater level is more than 40 m, and in some areas, it is between 20 and 40 m. The high-vulnerability areas of seawater intrusion are mainly distributed in the coastal areas of the Jiangmen-Zhuhai-Zhongshan-Guangzhou-Dongguan-Shenzhen area. The distance to shore is within 10 km in most of the high-vulnerability areas of seawater intrusion, and the groundwater in these areas has been generally affected by seawater intrusion. The groundwater level in the southern coastal area of Jiangmen is more than 2 m below sea level.

The medium-vulnerability areas of the geo-environment are mainly distributed in delta plains and coastal areas. In tablelands, hilly areas, and low mountainous areas, the medium-vulnerability areas are mainly distributed along faults. The low-vulnerability areas of the geo-environment are concentrated in tablelands, hilly areas, and low

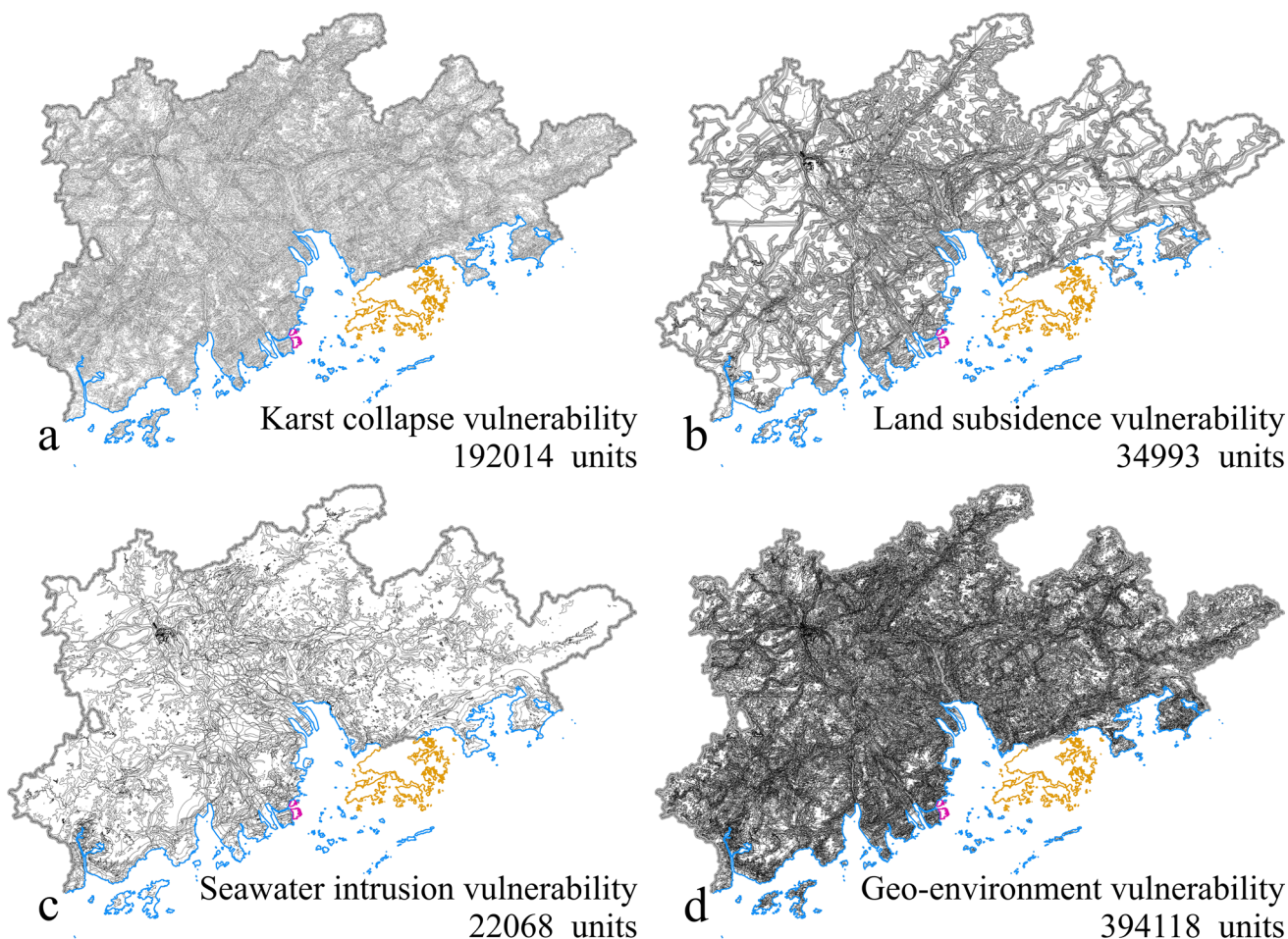


Fig. 4 Projection maps of vulnerability assessment units of geo-environmental issues and geo-environment: **a** karst collapse vulnerability, **b** land subsidence vulnerability, **c** seawater intrusion vulnerability, and **d** geo-environment vulnerability

Table 2 Results of vulnerability assessment of geo-environmental issues and geo-environment

Result of vulnerability assessment			High	Medium	Low	Extremely low
Karst collapse	AHP	Area (km ²)	326.60	1212.62	1759.09	38,399.69
		Number of karst collapse	8	46	19	49
	VW-AHP	Area (km ²)	1147.46	3787.81	9782.99	26,979.74
		Number of karst collapse	58	31	20	13
Land subsidence	AHP	Area (km ²)	438.53	2897.32	7260.95	31,101.23
		Number of land subsidence	4	40	27	8
	VW-AHP	Area (km ²)	2311.78	4236.26	9447.02	25,702.94
		Number of land subsidence	43	24	11	1
Seawater intrusion	AHP	Area (km ²)	630.01	1585.87	1914.80	37,375.10
		Area of seawater intrusion (km ²)	630.01	1567.71	1788.31	879.00
	VW-AHP	Area (km ²)	1399.12	2063.93	4711.35	33,523.60
		Area of seawater intrusion (km ²)	1352.93	1593.57	1413.94	504.64
Geo-environment	VW-AHP	Area (km ²)	4107.67	6599.02	11,846.08	19,145.23

mountainous areas of Huizhou, Zhaoqing, and Zhongshan, and scattered in other areas, roughly along the river. The extremely low–vulnerability areas of the geo-environment are widely distributed in tablelands, hilly areas, and low mountainous areas. There are very few soluble rocks and soft soil stratum in these areas. The depth of groundwater level is within 3 m, and the distance to shore is more than 2.5 km, so there are few geo-environmental issues.

Ecological environment function

Groundwater-dependent ecosystems (GDEs) are part of the environment and are ecosystems that are dependent on the permanent or temporary existence or impact of groundwater (Bekesi and Hodges 2006). Part or all of the water requirements of GDEs depend on groundwater to maintain their structure, composition, and function (Munch and Conrad 2007). GDEs play a vital role in the economy and environment of coastal areas (Paz et al. 2020). Groundwater input can support or compensate for surface water input to maintain GDEs in coastal areas (Erostate et al. 2020). The exploitation of groundwater has an impact on the groundwater level, thereby affecting the water source of GDEs. Therefore, the distribution of GDEs is used as an assessment indicator of the ecological environment function. In the study area, mangrove, protection forest, and economic forest as GDEs need to be protected (Fig. 3g). The development of groundwater should not have a negative impact on GDEs. The distribution data of GDEs is provided by Wuhan Center of Geological Survey.

On the other hand, the decrease of groundwater level caused by excessive exploitation of groundwater may lead to a decrease in vegetation coverage. Considering that vegetation coverage is an important indicator affecting soil erosion, the distribution of soil erosion is used as another assessment indicator of the ecological environment function (Pournader et al. 2018; Roy and Saha 2021; Sholagberu et al. 2019). The relevant data of soil erosion is provided by Wuhan Center of Geological Survey. Soil erosion occurred in low mountainous areas, hilly areas, tablelands, wasteland areas, and

mining areas with sparse vegetation, distributed in fragments (Fig. 3h).

Assessment of groundwater sustainable development

Before the assessment of groundwater sustainable development, the resource supply function, geo-environment stability function, and ecological environment function of groundwater are classified (Table 3). Specifically, the resource supply function is classified into three levels: good (Ra), general (Rb), and poor (Rc) according to groundwater quantity and quality, while the geo-environment stability function is classified into three levels: good (Ga), general (Gb), and poor (Gc) according to the geo-environment vulnerability. Based on the distribution of GDEs and soil erosion, the ecological environment function is classified into two levels: good (Ea) and poor (Eb).

The development of groundwater should be based on the protection of the ecological environment, and attention should be paid to maintaining the stability of the geo-environment. On this basis, combined with the groundwater quality and quantity, the groundwater supply area and the MGE are determined (CGS 2006; MWR 2005). The specific principles that should be followed in the assessment of groundwater sustainable development are shown in Fig. 5.

The study area is divided into 34,226 assessment units (Fig. 6). According to the above principles, the distribution areas of GDEs and soil erosion that need to be protected are determined as the ecological protection areas. Due to the high possibility of the occurrence of geo-environmental issues, the high–vulnerability areas of the geo-environment are determined as vulnerable geo-environment areas. In addition to these subareas, areas with large groundwater quantity, good groundwater quality, and the extremely low possibility of the occurrence of geo-environmental issues caused by groundwater development are identified as concentrated groundwater supply areas. The areas where groundwater does not meet the needs of utilization due to low quantity and poor quality are determined to be unsuitable to exploit groundwater areas. The remaining areas are

Table 3 Classification standards for the functions of groundwater

Function	Indicator	Good	General	Poor
Resource supply function	Groundwater quantity	$MGE > 300,000 \text{ m}^3/(\text{a}\cdot\text{km}^2)$	Neither R_a nor R_c	$MGE < 100,000 \text{ m}^3/(\text{a}\cdot\text{km}^2)$
	Groundwater quality	Classes I–III		Class V
Geo-environmental stability function	Geo-environment vulnerability	Extremely low–vulnerability area	Medium- and low-vulnerability area	High vulnerability area
Ecological environment function	GDEs	The distribution area of GDEs		The others
	Soil erosion	The distribution area of soil erosion		

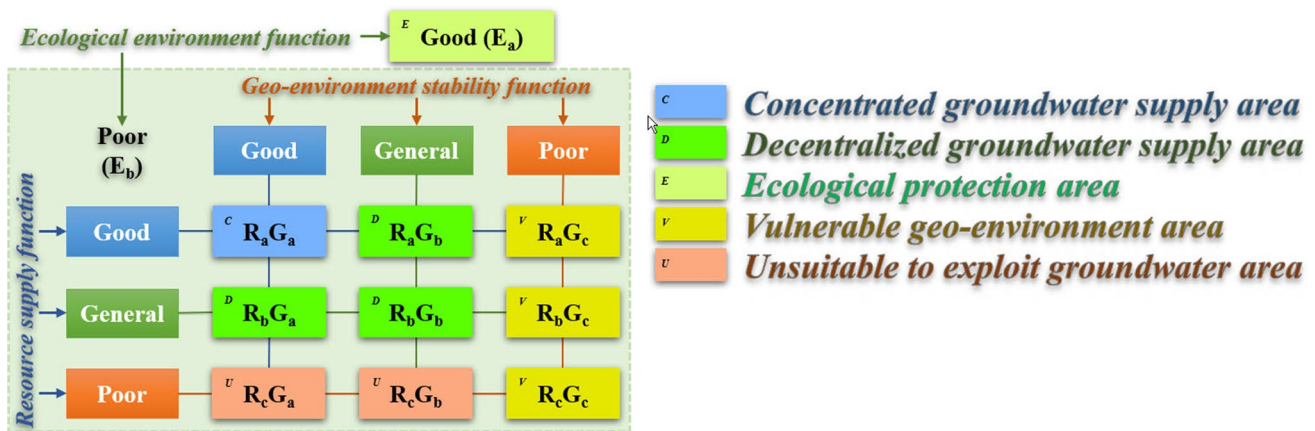


Fig. 5 Principles for the assessment of groundwater sustainable development

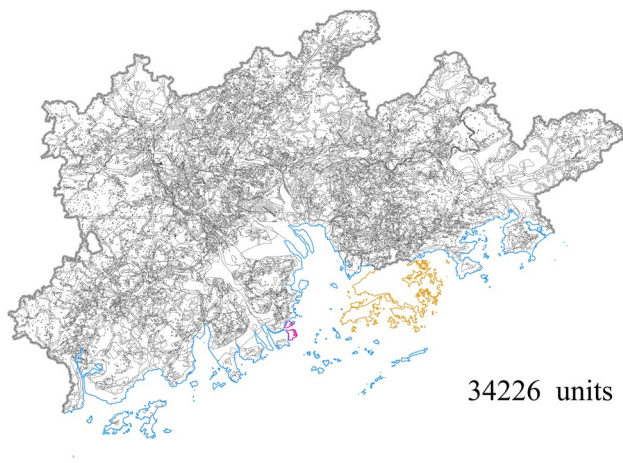


Fig. 6 Projection map of assessment units of groundwater sustainable development

identified as decentralized groundwater supply areas. The assessment results of groundwater sustainable development in the study area are shown in Fig. 7.

Ecological protection areas (8659.34 km²) are concentrated in three areas, namely, the Dongguan-Shenzhen area, the Jiangmen-Zhuhai-Zhongshan area, and the junction area of Jiangmen and Foshan. Besides, ecological protection areas are scattered in other areas. Vulnerable geo-environment areas (3726.86 km²) are mainly distributed in delta plains, river terraces, marine plains, and coastal areas of Jiangmen and Zhuhai. Concentrated groundwater supply areas (9160.36 km²) are mainly distributed in the tablelands, hilly areas, and low mountainous areas of Jiangmen, Zhaoqing, Guangzhou, and Huizhou. Unsuitable to exploit groundwater areas (42.74 km²) are located in the central part of Zhuhai, with a small area. The remaining areas in the study area are all decentralized groundwater supply areas (20,108.70 km²).

Discussions

Relationship between assessment results and functions of groundwater

The assessment of groundwater sustainable development is based on the resource supply function, geo-environment stability function, and ecological environment function of groundwater. Therefore, the assessment results are closely related to the groundwater quality and quantity, the geo-environment stability, and the distribution of GDEs and soil erosion.

Ecological protection areas are composed of the distribution areas of GDEs and soil erosion, which can be divided into three subareas (Fig. 7). Subarea I is the distribution area of GDEs and soil erosion. The main vegetation is protection forest and economic forest. The distribution areas of soil erosion are concentrated in Shenzhen, but scattered in other areas. Subarea II is the distribution area of GDEs. The areas where soil erosion occurred are relatively small and extremely scattered. Subarea III is also the distribution area of GDEs. Protection forest and economic forest are the main vegetations, and mangrove is only distributed in the northeast of Jiangmen, with a small area. Soil erosion only occurred sporadically in the northeast of Jiangmen. In addition to the above three subareas, there are also scattered distribution areas of GDEs and soil erosion in Huizhou, Guangzhou, and Zhaoqing. In ecological protection areas, the exploitation of groundwater should be prohibited.

The high-vulnerability areas of the geo-environment without distribution of GDEs and soil erosion are identified as vulnerable geo-environment areas, which can be divided into three subareas (Fig. 7). Subarea A is mainly the high-vulnerability area of karst collapse and land subsidence. Carbonate rock, sandstone, and sandy conglomerate are widely

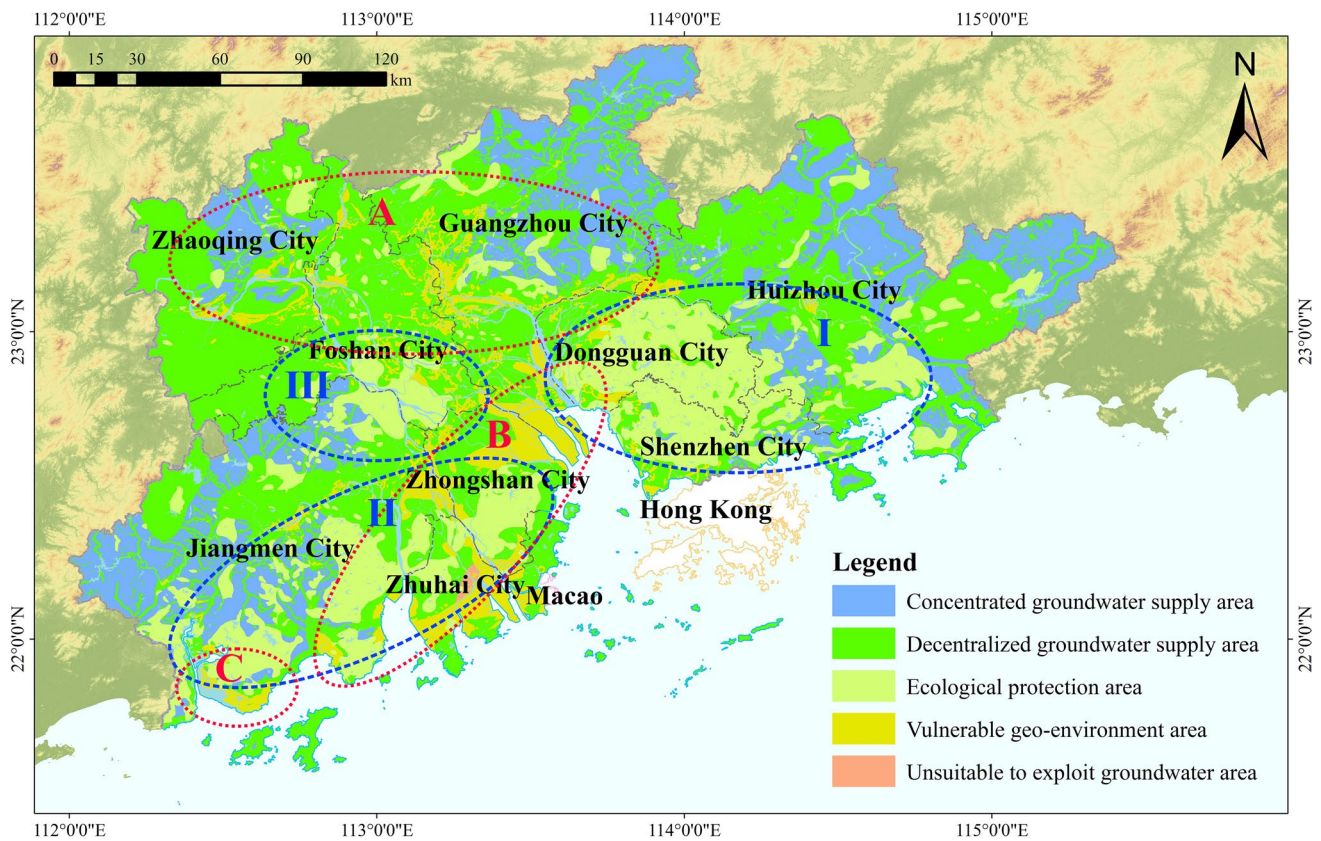


Fig. 7 Subarea map of groundwater sustainable development in the study area

distributed. The thickness of overlying layer is generally less than 5 m and the depth of groundwater level is generally greater than 20 m. Subarea B is mainly the high-vulnerability area of land subsidence and seawater intrusion. The TDS of groundwater is mostly greater than 1 g/L, which is greatly affected by seawater intrusion due to the close distance to shore. Soft soil stratum with a thickness of more than 20 m is widely distributed in subarea B. Subarea C is mainly the high-vulnerability area of seawater intrusion. The distance to shore is generally within 5 km, and the groundwater level is low, even more than 2 m below sea level. Due to severe seawater intrusion, the TDS of groundwater is more than 10 g/L. In addition to the above three subareas, there are also scattered vulnerable geo-environment areas in the central part of Jiangmen and the central part of Huizhou. A variety of geo-environmental issues occurred in these areas. If the water demand has been met, exploitation of groundwater is not recommended in vulnerable geo-environment areas. Otherwise, only decentralized, small-scale exploitation of groundwater can be allowed.

Concentrated groundwater supply areas are located in the tablelands, hilly areas, and low mountainous areas of Jiangmen, Zhaoqing, Guangzhou, and Huizhou, with a large area (Fig. 7). Groundwater with large quantity

($MGE > 30 \times 10^4 \text{ m}^3/(\text{a} \cdot \text{km}^2)$) and good quality (classes I–III) can be used as a source for domestic, industrial, and agricultural water. Due to the extremely low-vulnerability of the geo-environment and the absence of the distribution areas of GDEs and soil erosion, the occurrence of geological and ecological problems is not easily caused by the development of groundwater. So centralized exploitation of groundwater can be allowed.

Unsuitable to exploit groundwater areas are located in the central part of Zhuhai, with a small area (Fig. 7). Due to the low groundwater quantity ($MGE < 10 \times 10^4 \text{ m}^3/(\text{a} \cdot \text{km}^2)$) and poor groundwater quality (class V), the exploitation of groundwater is not recommended.

The remaining areas in the study area are all decentralized groundwater supply areas (Fig. 7). Groundwater with general quantity and quality in most areas can be exploited in a variety of ways, such as pumped wells. Groundwater can only be used as a source of agricultural water, but it can be used as drinking water after proper purification treatment. Due to the existence of medium- and low-vulnerability areas of geo-environment, the occurrence of geo-environmental issues should be considered in the exploitation of groundwater.

Comparison of AHP model and VW-AHP model

In this study, a VW-AHP model that combines AHP and variable weight theory is used in the vulnerability assessment of geo-environmental issues. Considering that the lower the rating of the indicator is, the greater the vulnerability of geological environmental issues is, so the penalty-type variable weight formula is used, that is, when the rating of the indicator is low, the variable weight of the indicator is increased. Compared with the results of using the AHP model, the area of each subarea has changed significantly with the results using the VW-AHP model. Specifically, the area of the extremely low–vulnerability areas decreases, and the area of other subareas increases, which is the result of adopting the penalty-type variable weight formula. For an assessment unit, the lower the rating of the indicator is, the greater the variable weight is, which leads to the lower CPI of the unit.

Three typical units were selected to illustrate the impact of the variable weight theory on the assessment results. Taking the 2318th unit in the assessment of karst collapse vulnerability as an example, using the AHP model, this unit is identified as a low-vulnerability area. But in fact, the ratings of *D* and *N* are 0.1. The value of *R* is 0.4. The ratings of *L*, *T*, *G*, and *F* are 1.0. The variable weights of *D* and *N* are greater than their constant weights, and the weights of other factors are the opposite. Compared with other assessment units, the penalty effect caused by the weight changes of the indicators of this unit is greater. Since the natural break classification method is used to classify the CPI, the 2318th unit is determined to be a high-vulnerability area using the VW-AHP model. In addition, the 520th unit in the assessment of land subsidence vulnerability is identified as a medium-vulnerability area using the AHP model. The variable weights of *T*, *D*, *F*, and *R* are greater than their constant weights, and the weight of *L* is the opposite. Compared with other assessment units, the penalty effect produced by the weight changes of the indicators of this unit is not sufficient to cause the change of vulnerability level. Finally, an example is given where the weight changes of the indicators lead to a lower vulnerability level. The 251th unit in the assessment of seawater intrusion vulnerability is identified as a high-vulnerability area using the AHP model. The rating of *T* is 0.1. The ratings of *D* and *I* are 0.4. The ratings of *A* and *G* are 0.7. Compared with the constant weights, the variable weight of *T* calculated by the VW-AHP model increases, while the variable weights of other factors decrease. Compared with other assessment units, the penalty effect caused by the weight changes of the indicators of this unit is smaller. Therefore, using the VW-AHP model, the 251th unit is determined to be a medium-vulnerability area.

The assessment results using the VW-AHP model indicate that 72.95% of karst collapse, 84.81% of land subsidence,

and 60.56% of seawater intrusion occurred in high- and medium-vulnerability areas. The ratios when the VHP model is adopted are 44.26%, 55.69%, and 45.17%, respectively (Table 2). The purpose of the assessment of geo-environment vulnerability based on the vulnerability assessment of geo-environmental issues is to assess the geo-environment stability function of groundwater. Therefore, the geo-environment stability can be maintained in the assessment of groundwater sustainable development, and the occurrence of geo-environmental issues can be avoided while exploiting groundwater. The assessment results using the VW-AHP model show that the area of high- and medium-vulnerability areas is larger and more geo-environmental issues occurred in these areas, compared with these using the AHP model (Table 2). From the perspective of maintaining the geo-environment stability, the assessment results using the VW-AHP model are helpful to protect the potential areas of the occurrence of geo-environmental issues in a larger area.

ROC curve

The receiver operating characteristic (ROC) curve can be used to quantitatively analyze the accuracy of the assessment model (Aghdam et al. 2017; Li et al. 2020a; Lucchese et al. 2021; Senouci et al. 2021). The area under the curve (AUC) value is between 0.1 and 1.0. The closer the AUC value is to 1.0, the more accurate the assessment model is, and an AUC value of 1.0 indicates that the model is the most accurate. If the assessment model is not more accurate than probability in predicting the occurrence of geo-environmental issues, the AUC value is less than 0.5 (Najafi et al. 2020). According to the AUC value, the accuracy of the assessment model is classified into excellent (0.9–1.0), very good (0.8–0.9), good (0.7–0.8), general (0.6–0.7), and poor (0.5–0.6). The AUC values of the assessment of karst collapse, land subsidence, and seawater intrusion vulnerability using the VW-AHP model are 0.864, 0.906, and 0.874, while the AUC values using the AHP model are 0.766, 0.856, and 0.861, respectively (Fig. 8). Therefore, in the assessment of karst collapse, land subsidence, and seawater intrusion vulnerability, the accuracies of the VW-AHP model are “very good,” “excellent,” and “very good,” while the accuracies of the AHP model are “good,” “very good,” and “very good,” indicating that the constant weights of the indicators are reasonable, but the variable weights determined by the variable weight theory of the indicators are more in line with the actual situation in the study area. The above conclusions indicate that the VW-AHP model is considered to be a better model than the AHP model for the vulnerability assessment of geo-environmental issues. The VW-AHP model can more accurately predict the possibility of the occurrence of geo-environmental issues, and the assessment results can better reflect the actual situation in the study area.

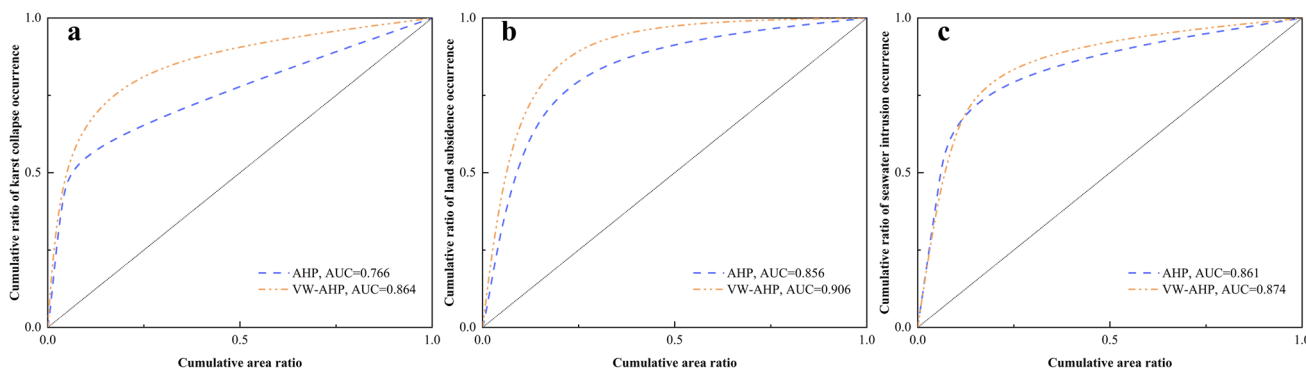


Fig. 8 ROC curves of vulnerability assessment of geo-environmental issues: **a** vulnerability assessment of karst collapse, **b** vulnerability assessment of land subsidence, and **c** vulnerability assessment of seawater intrusion

Single-indicator sensitivity analysis

Single-indicator sensitivity analysis can be used to check the spatial importance of each indicator in the CPI calculation (Yang et al. 2017). The calculation method of effective weight is shown in Eq. 12.

$$W_i = \frac{r_i \cdot w_i}{CPI} \tag{12}$$

In Eq. 12, W_i is the effective weight of the indicator. r_i and w_i are the rating and variable weight of the indicator, respectively. CPI represents the comprehensive index of the vulnerability of geo-environmental issues.

The analysis result shows that the effective weights of the indicators are close to the theoretical weights, indicating

that the accuracy of the VW-AHP model is relatively high (Table 4). In Table 4, the theoretical weight is the constant weight calculated by the AHP model. In the assessment of karst collapse vulnerability, the effective weights of L , D , and G are greater than the theoretical weights, and the weights of other indicators are opposite. The effective weights of D and T are 25.39% and 21.07%, and the theoretical weights are 17.21% and 23.81%, respectively. The effective weights and theoretical weights of the above two indicators are relatively large, which illustrates the importance of the data accuracy of the two indicators in the assessment of karst collapse vulnerability. Among them, the largest effective weight of D indicates that D has the greatest impact on the karst collapse vulnerability. In the assessment of land subsidence vulnerability, the effective weight and theoretical

Table 4 Results of single-indicator sensitivity analysis

Geo-environmental issue	Indicator	Theoretical weight (%)				Effective weight (%)			
		Max	Min	Mean	SD	Max	Min	Mean	SD
Karst collapse	L	54.60	4.80	15.52	8.73	19.87	10.74	15.70	1.62
	D	66.41	5.47	17.21	11.12	31.76	16.51	25.39	2.74
	T	61.97	5.63	23.81	15.33	27.09	15.00	21.07	3.24
	G	48.46	2.92	12.06	9.42	17.29	8.59	13.25	1.84
	N	43.18	2.78	13.58	9.57	13.88	7.06	10.20	1.58
	F	34.74	1.76	9.11	7.38	10.42	5.05	7.63	1.24
Land subsidence	R	32.27	1.60	8.72	6.90	9.30	4.55	6.77	1.10
	T	78.91	8.59	33.18	17.56	48.45	27.23	37.51	4.48
	D	54.75	2.95	16.06	12.12	23.31	10.79	16.29	2.60
	L	62.84	4.08	22.84	15.62	29.82	14.47	20.92	3.46
	F	48.02	2.58	13.79	10.32	17.97	8.46	12.70	2.07
Seawater intrusion	R	48.02	2.67	14.12	10.32	17.32	8.46	12.58	2.01
	A	29.36	1.03	7.76	6.89	9.45	3.99	6.15	1.17
	G	69.19	5.34	21.84	13.29	36.07	18.34	27.39	3.43
	D	54.56	2.93	19.17	13.07	23.18	10.72	15.54	2.57
	I	81.95	12.42	40.46	17.02	50.82	31.23	41.19	4.31
T	40.48	1.77	10.77	8.56	14.20	6.37	9.73	1.56	

weight of *T* are 37.51% and 33.18%, and the effective weight and theoretical weight of *D* are 16.29% and 16.06%, respectively. The effective weights of these two indicators are greater than the theoretical weights. The effective weights of the other indicators are less than the theoretical weights. The effective weight and theoretical weight of *T* are the largest, indicating that this indicator has the greatest impact on the land subsidence vulnerability. Therefore, the acquisition of detailed information of *T* is very important for the assessment of land subsidence vulnerability. In the assessment of seawater intrusion vulnerability, the effective weights of *G* and *I* are greater than the theoretical weights. The effective weights of other indicators are less than the theoretical weights. The effective weight of *I* is the largest, indicating that this indicator has the greatest impact on seawater intrusion vulnerability, and the data accuracy of this indicator is very important for the assessment of seawater intrusion vulnerability.

Suggestions for groundwater sustainable development

The purpose of this study is to provide a reference plan for groundwater sustainable development in the study area.

In the study area, there are 21 groundwater source protection areas, where the groundwater is mainly carbonate rock fissure-cave water and loose sediment pore water, most of which are distributed in plains, river terraces, and tablelands (Fig. 9). Based on the assessment results, several suggestions on groundwater sustainable development were put forward. Most of the groundwater source protection areas are located in concentrated groundwater supply areas and decentralized groundwater supply areas, but there are ecological protection areas and vulnerable geo-environment areas in some groundwater source protection areas. Groundwater source protection areas are concentrated in the northwest, southwest, and east of the study area.

In the northwest of the study area, three groundwater source protection areas, named Conghua-Shengang, Jianggu-Sihui, and Lubu, are basically located in concentrated groundwater supply areas and decentralized groundwater supply areas. There is no ecological protection area that needs special attention, and the possibility of the occurrence of geo-environmental issues caused by the exploitation of groundwater is relatively small. Therefore, reasonable exploitation can be continued according to water demand, groundwater quality, and groundwater quantity. As for the Sanshui-Longjiang groundwater source protection area,

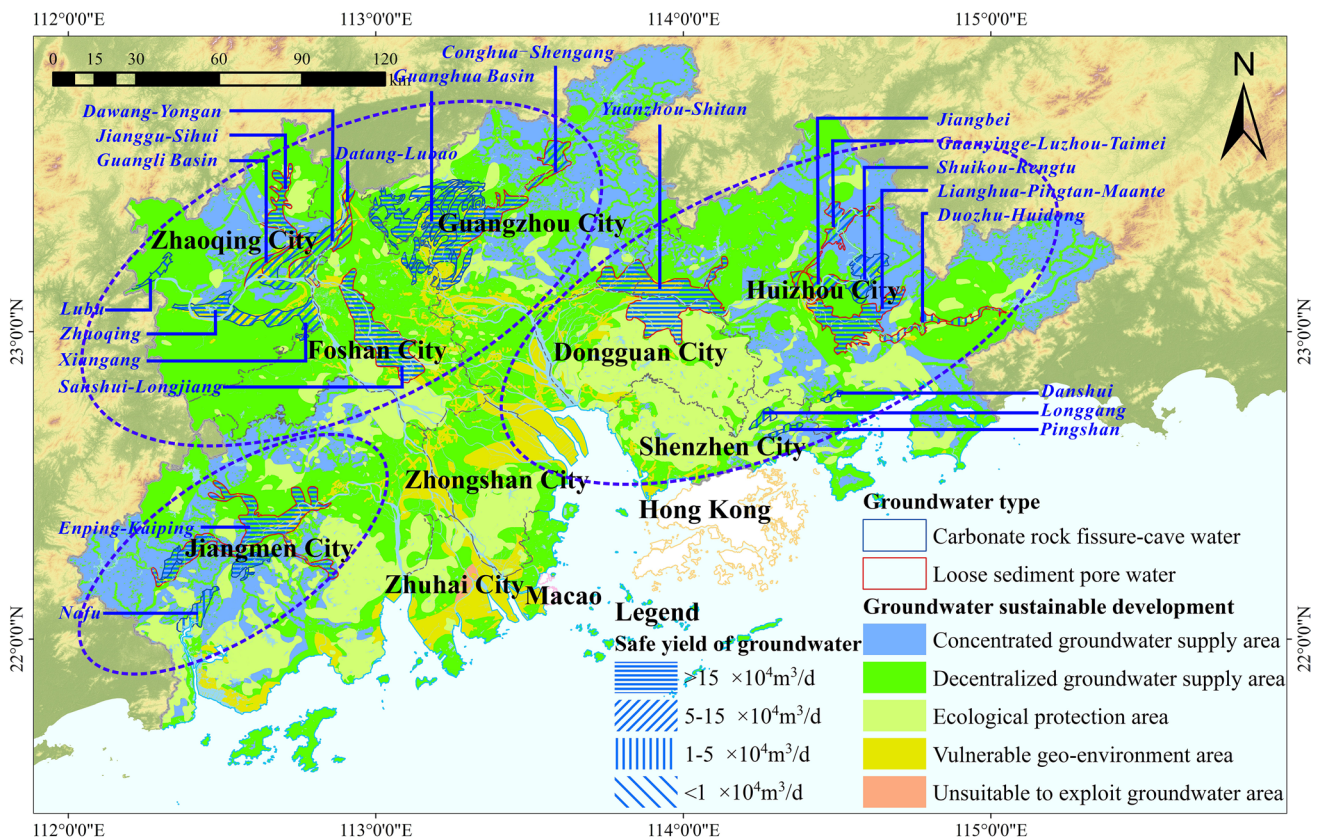


Fig. 9 Distribution map of groundwater source protection areas in the study area

there are scattered areas of vulnerable geo-environment areas and distribution areas of soil erosion in the middle of the protection area and distribution areas of GDEs in the south of the protection area. Attention should be paid to the possibility of the occurrence of karst collapse and land subsidence caused by the exploitation of groundwater in this protection area, and the impact on the ecological environment should also be paid attention to. In other groundwater source protection areas, during the exploitation of groundwater, attention should be paid to the occurrence of geo-environmental issues such as karst collapse and land collapse due to the existence of vulnerable geo-environment areas.

In the southwest of the study area, in the northeastern part of the Enping-Kaiping groundwater source protection area, there are high-vulnerability areas of karst collapse, and attention should be paid to the impact of the exploitation of groundwater on the occurrence of karst collapse. There are ecological protection areas in the southwestern part of the Nafu groundwater source protection area. The impact on GDEs is an important issue that should be considered during the exploitation of groundwater.

In the east of the study area, there are ecological protection areas in Duozhu-Huidong, Danshui, Longgang, and Pingshan groundwater source protection areas, so the main task is to protect the ecological environment. Due to the existence of vulnerable geo-environment areas in the Yuanzhou-Shitan groundwater source protection area, the karst collapse that may be induced by exploitation of groundwater and the impact on GDEs should be paid attention to. In other groundwater source protection areas, groundwater can be exploited as needed.

Improvements of methods and database

There are many debatable points in many aspects of this study from an objective point of view. Due to the limited accuracy of the data provided by Wuhan Center of Geological Survey, the division of groundwater quantity of the study area is based on the administrative area, which is not closely integrated with the hydrogeological conditions. Due to the lack of long-term observational data of groundwater level, the change of groundwater level was not used as an indicator for the vulnerability assessment of karst collapse and land subsidence. Some alternative indicators, such as groundwater abundance and depth of groundwater level, were adopted. The GALDIT method is widely used in the assessment of seawater intrusion. Some indicators can be added or modified to apply to areas with complex hydrogeological conditions. For example, electric conductivity is used as an alternative indicator for the impact of the existing status of seawater intrusion (Chang et al. 2019). Kazakis et al. (2019) proposed the GALDIT-SUSI method, as a modification of

the GALDIT method, adding six indicators to describe the “Superficial Seawater Intrusion (SUSI),” and applied the method in Greece and Italy. The GALDIT method can also be combined with other methods. For example, it can be combined with the groundwater quality index to identify groundwater types (Ayed et al. 2018; Trabelsi et al. 2016). Besides, in the assessment of the ecological environment function of groundwater, only two factors, the distribution of GDEs and the distribution of soil erosion, were considered, and only two ecosystems, mangrove and protection forest and economic forest, were identified as GDEs. In fact, coastal ecosystems and riparian ecosystems are also areas that need to be protected (Huang et al. 2020; Wada et al. 2020; Xu and Su 2019). However, considering that surface water is the main water source, these areas were not identified as ecological protection areas.

The VW-AHP model was used to assess the vulnerability of geo-environmental issues. The determination of the weights of indicators in this model depends on the subjective experience of decision-makers and experts. To explore the establishment of a more objective assessment method, some other methods can be considered, such as the logistic regression model (Du et al. 2019), weighted spatial probability model (Elmahdy et al. 2016), BP neural network method (Li et al. 2020c), and random forest method (Ebrahimi et al. 2020). At present, the research mainly focuses on the prediction of the exploitation potential of groundwater and the delineation of recharge areas of groundwater. There is still no universally recognized method for the assessment of groundwater sustainable development. An assessment method based on the resource supply function, the geo-environment stability function, and the ecological environment function was proposed. With this method, the determination of the groundwater supply area and the protection of the geo-environment and ecological environment were unified. The assessment results provided a feasible scheme for groundwater management in coastal cities. However, some issues, such as the geo-environmental issues induced by the dynamic changes of groundwater level and the impact of groundwater quality and quantity on complex ecosystems, are still worthy of further research.

Conclusions

In this study, a VW-AHP model that combines AHP and variable weight theory was used to assess the groundwater sustainable development in the Pearl River Delta. Based on the resource supply function, the geo-environment stability function, and the ecological environment function of groundwater, the groundwater in the Pearl River Delta was divided into concentrated groundwater supply area (9160.36 km²) and decentralized groundwater supply

area (20,108.70 km²), ecological protection area (8659.34 km²), vulnerable geo-environment area (3726.86 km²), and unsuitable to exploit groundwater area (42.74 km²). Based on the assessment results, suggestions for the exploitation of groundwater in each subarea were proposed. This study can also be used as an example of the assessment of groundwater sustainable development in coastal cities.

Groundwater quantity and quality were used as indicators for the assessment of the resource supply function. The geo-environment stability function was described by the geo-environment vulnerability which was described by the vulnerability of geo-environmental issues such as karst collapse, land subsidence, and seawater intrusion. The ecological environment function was determined by the distribution of GDEs and soil erosion.

In the vulnerability assessment of geo-environmental issues, the penalty-type variable weight formula was used to adjust the weights of indicators, which leads to a decrease in the area of the extremely low–vulnerability areas and an increase in the area of other subareas. The AUC value showed that the results of using the VW-AHP model were more in line with the actual situation in the Pearl River Delta than those of using the AHP model. The results of single-indicator sensitivity analysis revealed the degree of influence of assessment indicators on the vulnerability of geo-environmental issues and also showed that the effective weights of the indicators were close to the theoretical weights, and the accuracy of the VW-AHP model was relatively high.

Taking the assessment results of groundwater sustainable development as references, suggestions were provided for the exploitation of groundwater in groundwater source protection areas in the Pearl River Delta.

Further research should be conducted on the determination of the weights of the assessment indicators of geo-environment vulnerability, the assessment method of the assessment of groundwater sustainable development, and the impact of the dynamic changes of groundwater level on the geo-environment and ecological environment.

Supplementary Information The online version contains supplementary material available at <https://doi.org/10.1007/s11356-021-16924-6>.

Acknowledgements The authors wish to thank the Wuhan Center of Geological Survey for data curation. The authors also thank Mr. Zuo Liu and Zechen Zhang for their assistance in the analysis and visualization. The authors are grateful to the editor and reviewers for their suggestions.

Author contribution Peng Huang: Conceptualization, methodology, formal analysis, writing—original draft preparation, visualization.

Chuanming Ma: Writing—review and editing.

Aiguo Zhou: Resources, data curation, funding acquisition.

Funding This work was supported by the Fundamental Research Funds for the Central University, China University of Geosciences (Wuhan) [No. CUGCJ1822].

Data availability Not applicable.

Declarations

Ethics approval and consent to participate Not applicable.

Consent for publication Not applicable.

Conflict of interest The authors declare no competing interests.

References

- Achour Y, Boumezbeur A, Hadji R, Chouabbi A, Cavaleiro V, Bendaoud E (2017) Landslide susceptibility mapping using analytic hierarchy process and information value methods along a highway road section in Constantine. Algeria Arab J Geosci 10(8):194. <https://doi.org/10.1007/s12517-017-2980-6>
- Adiat KAN, Nawawi MNM, Abdullah K (2012) Assessing the accuracy of GIS-based elementary multi criteria decision analysis as a spatial prediction tool - a case of predicting potential zones of sustainable groundwater resources. J Hydrol 440:75–89. <https://doi.org/10.1016/j.jhydrol.2012.03.028>
- Aghdam IN, Pradhan B, Panahi M (2017) Landslide susceptibility assessment using a novel hybrid model of statistical bivariate methods (FR and WOE) and adaptive neuro-fuzzy inference system (ANFIS) at southern Zagros Mountains in Iran. Environ Earth Sci 76(6):237. <https://doi.org/10.1007/s12665-017-6558-0>
- Allafta H, Opp C, Patra S (2021) Identification of groundwater potential zones using remote sensing and GIS techniques: a case study of the Shatt Al-Arab Basin. Remote Sens 13(1):112. <https://doi.org/10.3390/rs13010112>
- Alley WM, Reilly TE, Franke OL (1999) Sustainability of ground-water resources U. S. Geological Survey Circular. United States Geological Survey, Denver, p 1186
- Almouctar MAS, Wu YP, Kumar A, Zhao FB, Mambu KJ, Sadek M (2021) Spatiotemporal analysis of vegetation cover changes around surface water based on NDVI: a case study in Korama basin, Southern Zinder. Niger Applied Water Science 11(1):4. <https://doi.org/10.1007/s13201-020-01332-x>
- Al-Zu'bi Y, Shatanawi M, Al-Jayoussi O, Al-Kharabsheh A (2002) Application of decision support system for sustainable management of water resources in the Azraq Basin – Jordan. Water International 27(4):532–541. <https://doi.org/10.1080/02508060208687040>
- Amano H, Iwasaki Y (2020) Land cover classification by integrating NDVI time series and GIS data to evaluate water circulation in Aso Caldera, Japan. Int J Environ Res Public Health 17(18):6605. <https://doi.org/10.3390/ijerph17186605>
- Amiri V, Nakhaei M, Lak R, Kholghi M (2016) Investigating the salinization and freshening processes of coastal groundwater resources in Urmia aquifer. NW Iran Environmental Monitoring and Assessment 188(4):233. <https://doi.org/10.1007/s10661-016-5231-5>
- Arabameri A, Saha S, Roy J, Tiefenbacher JP, Cerda A, Biggs T, Pradhan B, Ngo PTT, Collins AL (2020) A novel ensemble computational intelligence approach for the spatial prediction of land subsidence susceptibility. Science of Total Environment 726:138595. <https://doi.org/10.1016/j.scitotenv.2020.138595>

- Asefi H, Zhang Y, Lim S, Maghrebi M, Shahparvari S (2020) A multi-criteria decision support framework for municipal solid waste landfill siting: a case study of New South Wales (Australia). *Environ Monit Assess* 192(11):682. <https://doi.org/10.1007/s10661-020-08565-y>
- Aslan V, Celik R (2021) Integrated GIS-based multi-criteria analysis for groundwater potential mapping in the Euphrates's Sub-Basin, Harran Basin. *Turkey Sustainability* 13(13):7375. <https://doi.org/10.3390/su13137375>
- Ayed B, Jmal I, Sahal S, Bouri S (2018) The seawater intrusion assessment in coastal aquifers using GALDIT method and groundwater quality index: the Djefara of Medenine coastal aquifer (Southeastern Tunisia). *Abadian Journal of Geosciences* 11(20):609. <https://doi.org/10.1007/s12517-018-3966-8>
- Bao JD, Zhang JD, Li F, Liu CY, Shi SP (2016) Social benefits of the mine occupational health and safety management systems of mines in China and Sweden based on a fuzzy analytic hierarchy process: a comparative study. *Journal of Intelligent Fuzzy Systems* 31(6):3113–3120. <https://doi.org/10.3233/JIFS-169197>
- Bekesi G, Hodges S (2006) The protection of groundwater dependent ecosystems in Otago. *New Zealand Hydrogeology Journal* 14(8):1696–1701. <https://doi.org/10.1007/s10040-006-0062-z>
- Besikci EB, Kececi T, Arslan O, Turan O (2016) An application of fuzzy-AHP to ship operational energy efficiency measures. *Ocean Eng* 121:392–402. <https://doi.org/10.1016/j.oceaneng.2016.05.031>
- Bian JM, Liu CH, Zhang ZZ, Wang R, Gao Y (2016) Hydro geochemical characteristics and health risk evaluation of nitrate in groundwater. *Pol J Environ Stud* 25(2):521–527. <https://doi.org/10.15244/pjoes/61113>
- Bordbar M, Neshat A, Javadi S (2019) Modification of the GALDIT framework using statistical and entropy models to assess coastal aquifer vulnerability. *Hydrological Sciences Journal- Journal Des Sciences Hydrological* 64(9):1117–1128. <https://doi.org/10.1080/02626667.2019.1620951>
- Bordbar M, Neshat A, Javadi S, Pradhan B, Aghamohammadi H (2020) Meta-heuristic algorithms in optimizing GALDIT framework: a comparative study for coastal aquifer vulnerability assessment. *J Hydrol* 585:124768. <https://doi.org/10.1016/j.jhydrol.2020.124768>
- Bui NT, Kawamura A, Bui DD, Amaguchi H, Bui DD, Truong NT, Nakagawa K (2018) Social sustainability assessment of groundwater resources: a case study of Hanoi. *Vietnam Ecological Indicators* 93:1034–1042. <https://doi.org/10.1016/j.ecolind.2018.06.005>
- Bui NT, Kawamura A, Bui DD, Amaguchi H, Bui DD, Truong NT, Do HHT, Nguyen CT (2019) Groundwater sustainability assessment framework: a demonstration of environmental sustainability index for Hanoi. *Vietnam Journal of Environmental Management* 241:479–487. <https://doi.org/10.1016/j.jenvman.2019.02.117>
- C. G. S., (1979) Synthetic hydrogeological map Republic of China. F-49 series scale 1:200,000. Guangzhou Geological Survey, Guangzhou (in Chinese)
- C. G. S., (1981) Synthetic hydrogeological map Republic of China. F-50 series scale 1:200,000. Guangzhou Geological Survey, Guangzhou (in Chinese)
- C. G. S., (2006) Technical requirements for the evaluation and zoning of groundwater function. China Geological Survey, Beijing
- C. G. S., (2012) Handbook of hydrogeology. Geological Publishing House, Beijing (in Chinese)
- Calligaris C, Devoto S, Galve JP, Zini L, Perez-Pena JV (2017) Integration of multi-criteria and nearest neighbour analysis with kernel density functions for improving sinkhole susceptibility models: the case study of Enemonzo (NE Italy). *Int J Speleol* 46(2):191–204. <https://doi.org/10.5038/1827-806X.46.2.2099>
- Chang SW, Chung IM, Kim MG, Tolera M, Koh GW (2019) Application of GALDIT in assessing the seawater intrusion vulnerability of Jeju Island, South Korea. *Water* 11(9):1824. <https://doi.org/10.3390/w11091824>
- Chen J (2012) Assessment of groundwater sustainability using multi-indicators in the Hohhot Plain. Chinese Academy of Geological Sciences, Beijing (in Chinese)
- Chen J, Zhang YL, Chen ZY, Nie ZL (2015) Improving assessment of groundwater sustainability with analytic hierarchy process and information entropy method: a case study of the Hohhot Plain, China. *Environmental Earth Sciences* 72:2353–2363. <https://doi.org/10.1007/s12665-014-3583-0>
- Chen W, Han HX, Huang B, Huang QL, Fu XD (2017) Variable-weighted linear combination model for landslide susceptibility mapping: case study in the Shennongjia Forestry District. *China Isprs International Journal of Geo-Information* 6(11):347. <https://doi.org/10.3390/ijgi6110347>
- Chen T, Xia J, Zou L, Hong S (2020) Quantifying the influences of natural factors and human activities on NDVI changes in the Hanjiang River Basin. *China Remote Sensing* 12(22):3780. <https://doi.org/10.3390/rs12223780>
- Cunliffe AM, Assmann JJ, Daskalova GN, Kerby JT, Myers-Smith IH (2020) Aboveground biomass corresponds strongly with drone-derived canopy height but weakly with greenness (NDVI) in a shrub tundra landscape. *Environ Res Lett* 15(12):125004. <https://doi.org/10.1088/1748-9326/aba470>
- Daneshvar MRM (2014) Landslide susceptibility zonation using analytical hierarchy process and GIS for the Bojnurd region, north-east of Iran. *Landslides* 11(6):1079–1091. <https://doi.org/10.1007/s10346-013-0458-5>
- Das S (2018) Geographic information system and AHP-based flood hazard zonation of Vaitarna basin, Maharashtra. *India Arabian Journal of Geosciences* 11(19):576. <https://doi.org/10.1007/s12517-018-3933-4>
- Das Gupta A, Onta PR (1997) Sustainable groundwater resources development. *Hydrol Sci J* 42(4):565–582. <https://doi.org/10.1080/02626669709492054>
- De Marinis P, Sali G (2020) Participatory analytic hierarchy process for resource allocation in agricultural development projects. *Eval Program Plann* 80:101793. <https://doi.org/10.1016/j.evalproglan.2020.101793>
- De Carvalho SCP, Carden KJ, Armitage NP (2009) Application of a sustainability index for integrated urban water management in Southern African cities: case study comparison - Maputo and Hermanus. *Water SA* 35(2):144–151
- De Waele J, Gutierrez F, Parise M, Plan L (2011) Geomorphology and natural hazards in karst areas: a review. *Geomorphology* 134(1–2):1–8. <https://doi.org/10.1016/j.geomorph.2011.08.001>
- Dilekoglu MF, Aslan V (2021) Determination of groundwater potential distribution of Ceylanpinar plain (Turkey) in Upper Mesopotamia by using geographical information techniques and Fuzzy-AHP with MCDM. *Water Supply, Early Access*. <https://doi.org/10.2166/ws.2021.268>
- Ding N (2018) Evaluation of groundwater resources and analysis of exploitation potential in Chahar Youyiqianqi-Jining District. China University of Geosciences, Beijing ((in Chinese))
- Domazatovic F, Sijeg A, Loncar N, Maric I (2019) Development of automated multicriteria GIS analysis of gully erosion susceptibility. *Appl Geogr* 112:102083. <https://doi.org/10.1016/j.apgeog.2019.102083>
- Dong HG, Huang CS, Chen W, Zhang HX, Zhi BF, Zhao XW (2012) The controlling factors of environment geology in the Pearl River Delta economic zone and an analysis of existing problems. *Geology in China* 39(2):539–550 (in Chinese)
- Drobinina E, Kovaleva T, Koriakina A (2020) The local variation of the overlying soils geotechnical properties in the karst susceptibility

- assessment. *Carbonates Evaporites* 35(3):79. <https://doi.org/10.1007/s13146-020-00615-3>
- Du GL, Zhang YS, Yang ZH, Guo CB, Yao X, Sun DY (2019) Landslide susceptibility mapping in the region of eastern Himalayan syntaxis, Tibetan Plateau, China: a comparison between analytical hierarchy process information value and logistic regression-information value methods. *Bull Eng Geol Env* 78(6):4201–4215. <https://doi.org/10.1007/s10064-018-1393-4>
- Gabrielsen P, Bosch P (2003) Environmental indicators: typology and use in reporting. E. E. A. Internal Working Paper. Copenhagen: European Environmental Agency
- Ebrahimi H, Feizizadeh B, Salmani S, Azadi H (2020) A comparative study of land subsidence susceptibility mapping of Tasuj plane, Iran, using boosted regression tree, random forest and classification and regression tree methods. *Environmental Earth Sciences* 79(10):223. <https://doi.org/10.1007/s12665-020-08953-0>
- Elmahdy SI, Marghany MM, Mohamed MM (2016) Application of a weighted spatial probability model in GIS to analyse landslides in Penang Island. *Malaysia Geomatics Natural Hazards & Risk* 7(1):345–359. <https://doi.org/10.1080/19475705.2014.904825>
- Erostate M, Huneau F, Garel E, Ghiotti S, Vystavna Y, Garrido M, Pasqualini V (2020) Groundwater dependent ecosystems in coastal Mediterranean regions: characterization, challenges and management for their protection. *Water Res* 172:115461. <https://doi.org/10.1016/j.watres.2019.115461>
- Fadhillah MF, Achmad AR, Lee CW (2020) Integration of InSAR time-series data and GIS to assess land subsidence along subway lines in the Seoul Metropolitan Area. *South Korea Remote Sensing* 12(21):3505. <https://doi.org/10.3390/rs12213505>
- Fidelibus MD, Gutierrez F, Spilotro G (2011) Human-induced hydrogeological changes and sinkholes in the coastal gypsum karst of Lesina Marina area (Foggia Province, Italy). *Eng Geol* 118(1–2):1–19. <https://doi.org/10.1016/j.enggeo.2010.12.003>
- G. H. S. T., (1981) Regional hydrogeological survey report. Guangdong Hydrogeological Second Team, Guangzhou
- Gao L, Ma CM, Wang QX, Zhou AG (2019) Sustainable use zoning of land resources considering ecological and geological problems in Pearl River Delta Economic Zone. *China Scientific Reports* 9:16052. <https://doi.org/10.1038/s41598-019-52355-7>
- Gholami V, Yousefi Z, Rostami HZ (2010) Modeling of ground water salinity on the Caspian Southern Coasts. *Water Resour Manage* 24(7):1415–1424. <https://doi.org/10.1007/s11269-009-9506-2>
- Gugulothu S, Dhakate R, Sreedhar K, Ramesh A, Saxena PR (2020) Geophysical and hydrochemical studies for sustainable development of groundwater resources in northwestern part of Telangana State. *India Journal of Earth System Science* 129(1):202. <https://doi.org/10.1007/s12040-020-01452-7>
- Guo X, Ma CM, Hu XJ, Yan W (2019) Application of groundwater functional zoning to coastal groundwater management: a case study in the plain area of Weifang City. *China Environmental Earth Sciences* 78(16):525. <https://doi.org/10.1007/s12665-019-8534-3>
- Gupta A, Castro-Fresno D, Lastra-Gonzalez P, Rodriguez-Hernandez J (2021) Selection of fibers to improve porous asphalt mixtures using multi-criteria analysis. *Construction and Building Materials* 266(Part A):121198. <https://doi.org/10.1016/j.conbuildmat.2020.121198>
- Hakim WL, Achmad AR, Eom J, Lee CW (2020a) Land subsidence measurement of Jakarta coastal area using time series interferometry with Sentinel-1 SAR data. *J Coastal Res* 102(sp1):75–81. <https://doi.org/10.2112/SI102-010.1>
- Hakim WL, Achmad AR, Lee CW (2020b) Land subsidence susceptibility mapping in Jakarta using functional and meta-ensemble machine learning algorithm based on time-series InSAR data. *Remote Sensing* 12(21):3627. <https://doi.org/10.3390/rs12213627>
- Hallal DD, Khelif ME, Zahouani S, Benamghar A, Haddad O, Ammari A, Lobo-Ferreira JP (2019) Application of the GALDIT method combined with geostatistics at the Bouteldja aquifer (Algeria). *Environmental Earth Sciences* 78(1):22. <https://doi.org/10.1007/s12665-018-8005-2>
- He W, Zhou J, Cheng H, Wang LY, Wei K, Wang WF, Li XH (2012) Validation of origins of tea samples using partial least squares analysis and Euclidean distance method with near-infrared spectroscopy data. *Spectrochim Acta Part A Mol Biomol Spectrosc* 86:399–404. <https://doi.org/10.1016/j.saa.2011.10.056>
- He KQ, Jia YY, Wang B, Wang RL, Luo HL (2013) Comprehensive fuzzy evaluation model and evaluation of the karst collapse susceptibility in Zaozhuang Region. *China Natural Hazards* 68(2):613–629. <https://doi.org/10.1007/s11069-013-0653-7>
- Hosseini SM, Parizi E, Ataie-Ashtiani B, Simmons CT (2019) Assessment of sustainable groundwater resources management using integrated environmental index: case studies across Iran. *Sci Total Environ* 676:792–810. <https://doi.org/10.1016/j.scitotenv.2019.04.257>
- Hou JM, Su C, Wang WS (2008) AHP methodology for partner selection in collaborative design. *International Symposium on Computer Science and Computational Technology* 2:674–677. <https://doi.org/10.1109/ISCSCCT.2008.359>
- Hou QX, Sun JC, Jing JH, Liu CY, Zhang Y (2018) A regional scale investigation on groundwater arsenic in different types of aquifers in the Pearl River Delta. *China Geofluids* 2018:2471295. <https://doi.org/10.1155/2018/3471295>
- Huang ZG, Zong YQ, Zhang WQ (2004) Coastal inundation due to sea level rise in the Pearl River Delta China. *Natural Hazards* 33(2):247–264. <https://doi.org/10.1023/B:NHAZ.0000037038.18814.b0>
- Huang GX, Liu CY, Sun JC, Zhang M, Jing JH, Li LP (2018) A regional scale investigation on factors controlling the groundwater chemistry of various aquifers in a rapidly urbanized area: a case study of the Pearl River Delta. *Sci Total Environ* 625:510–518. <https://doi.org/10.1016/j.scitotenv.2017.12.322>
- Huang F, Chunyu XZ, Zhang DR, Chen X, Ochoa CG (2020) A framework to assess the impact of ecological water conveyance on groundwater-dependent terrestrial ecosystems in arid inland river basins. *Sci Total Environ* 709:136155. <https://doi.org/10.1016/j.scitotenv.2019.136155>
- I. H. E. G., (2010) Investigation and evaluation report on groundwater pollution in the Pearl River Delta. Shijiazhuang, Institute of Hydrogeology and Environmental Geology Chinese Academy of Geological Sciences (in Chinese)
- Janssen R (1992) Multiobjective decision support for environmental management. Kluwer Academic Publishers, Dordrecht
- Javanbarg MB, Scawthorn C, Kiyono J, Shahbodaghkhan B (2012) Fuzzy AHP-based multicriteria decision making systems using particle swarm optimization. *Expert Syst Appl* 39(1):960–966. <https://doi.org/10.1016/j.eswa.2011.07.095>
- Javidan N, Kaviani A, Pourghasemi HR, Conoscenti C, Jafarian Z, Rodrigo-Comino J (2021) Evaluation of multi-hazard map produced using MaxEnt machine learning technique. *Sci Rep* 11(1):6496. <https://doi.org/10.1038/s41598-021-85862-7>
- Jha MK, Chowdhury VM, Chowdhury A (2010) Groundwater assessment in Salboni Block, West Bengal (India) using remote sensing, geographical information system and multi-criteria decision analysis techniques. *Hydrogeolgy Journal* 18(7):1713–1728. <https://doi.org/10.1007/s10040-010-0631-z>
- Jhariya DC, Kumar T, Gobinath M, Diwan P, Kishore N (2016) Assessment of groundwater potential zone using remote sensing, GIS and multi criteria decision analysis techniques. *J Geol Soc India* 88(4):481–492. <https://doi.org/10.1007/s12594-016-0511-9>
- Jia YF, Xi, B. D., Jiang, Y. H., Guo, H. M., Yang, Y., Lian, X. Y., Han, S. B., (2018) Distribution, formation and human-induced

- evolution of geogenic contaminated groundwater in China: a review. *Sci Total Environ* 643:967–993. <https://doi.org/10.1016/j.scitotenv.2018.06.201>
- Jia C, Zhang YW, Han JM, Xu XQ (2017) Susceptibility area regionalization of land subsidence based on extenics theory. *Cluster Computing—the Journal of Networks Software Tools and Applications* 20(1):53–66. <https://doi.org/10.1007/s10586-016-0720-4>
- Jia XY, O'Connor D, Hou DY, Jin YL, Li GH, Zheng CM, Ok YS, Tsang DCW, Lu J (2019) Groundwater depletion and contamination: spatial distribution of groundwater resources sustainability in China. *Sci Total Environ* 672:551–562. <https://doi.org/10.1016/j.scitotenv.2019.03.457>
- Jiang XZ, Lei MT, Zhao HQ (2019) Review of the advanced monitoring technology of groundwater-air pressure (enclosed potentiometric) for karst collapse studies. *Environmental Earth Sciences* 78(24):701. <https://doi.org/10.1007/s12665-019-8716-z>
- Jothibasu A, Anbazhagan S (2018) Hydrogeological assessment of the groundwater aquifers for sustainability state and development planning. *Environmental Earth Sciences* 77(3):88. <https://doi.org/10.1007/s12665-017-7211-7>
- Kang MG, Lee GM (2011) Multicriteria evaluation of water resources sustainability in the context of watershed management. *J Am Water Resour Assoc* 47(4):813–827. <https://doi.org/10.1111/j.1752-1688.2011.00559.x>
- Karamouz M, Teymori J, Rahimi R, Olyaei MA, Mohammadpour P (2018) The impact of artificial groundwater recharge on water resources sustainability. *World Environmental and Water Resources Congress* 92–102
- Kazakis N, Spiliotis M, Voudouris K, Pliakas FK, Papadopoulos B (2018) A fuzzy multicriteria categorization of the GALDIT method to assess seawater intrusion vulnerability of coastal aquifers. *Sci Total Environ* 621:524–534. <https://doi.org/10.1016/j.scitotenv.2017.11.235>
- Kazakis N, Busico G, Colombani N, Mastrocicco M, Pavlou A, Voudouris K (2019) GALDIT-SUSI a modified method to account for surface water bodies in the assessment of aquifer vulnerability to seawater intrusion. *J Environ Manage* 235:257–265. <https://doi.org/10.1016/j.jenvman.2019.01.069>
- Kumar R, Anbalagan R (2015) Landslide susceptibility zonation in part of Tehri reservoir region using frequency ratio, fuzzy logic and GIS. *J Earth Syst Sci* 124(2):431–448. <https://doi.org/10.1007/s12040-015-0536-2>
- Kumru M, Kumru Y (2014) Analytic hierarchy process application in selecting the mode of transport for a logistics company. *J Adv Transp* 48(8):947–999. <https://doi.org/10.1002/atr.1240>
- Langat PK, Kumar L, Koech R (2020) GIS-based geomorphometric analysis for potential applications in reversing land and biosystem degradation. *Environ Monit Assess* 192(10):668. <https://doi.org/10.1007/s10661-020-08640-4>
- Lee GKL, Chan EHW (2008) The analytic hierarchy process (AHP) approach for assessment of urban renewal proposals. *Soc Indic Res* 89(1):155–168. <https://doi.org/10.1007/s11205-007-9228-x>
- Li WB, Fan XM, Huang FM, Chen W, Hong HY, Huang JS, Guo ZZ (2020a) Uncertainties analysis of collapse susceptibility prediction based on remote sensing and GIS: influences of different data-based models and connections between collapses and environmental factors. *Remote Sensing* 12(24):4134. <https://doi.org/10.3390/rs12244134>
- Li X, Tang CY, Cao YJ, Li D (2020b) A multiple isotope (H, O, N, C and S) approach to elucidate the hydrochemical evolution of shallow groundwater in a rapidly urbanized area of the Pearl River Delta. *China Science Og the Total Environment* 724:137930. <https://doi.org/10.1016/j.scitotenv.2020.137930>
- Li ZY, Wang YC, Olgun CG, Yang SQ, Jiao QL, Wang MT (2020c) Risk assessment of water inrush caused by karst cave in tunnels based on reliability and GA-BP neural network. *Geomat Nat Haz Risk* 11(1):1212–1232. <https://doi.org/10.1080/19475705.2020.1785956>
- Lin CJ, Zhang M, Zhou ZQ, Li LP, Shi SS, Chen YX, Dai WJ (2020) A new quantitative method for risk assessment of water inrush in karst tunnels based on variable weight function and improved cloud model. *Tunn Undergr Space Technol* 95:103136. <https://doi.org/10.1016/j.tust.2019.103136>
- Liu SL, Li WP (2019) Indicators sensitivity analysis for environmental engineering geological patterns caused by underground coal mining with integrating variable weight theory and improved matter-element extension model. *Sci Total Environ* 686:606–618. <https://doi.org/10.1016/j.scitotenv.2019.04.393>
- Liu F, Huang GX, Sun JC, Jing JH, Zhang Y (2014) Distribution of arsenic in shallow aquifers of Guangzhou region, China: natural and anthropogenic impacts. *Water Qual Res J Can* 49(4):354–371. <https://doi.org/10.2166/wqrjc.2014.014>
- Liu F, Sun JC, Wang J, Zhang Y (2017) Groundwater acidification in shallow aquifers in Pearl River Delta, China: distribution, factors, and effects. *Geochim J* 51(4):373–384. <https://doi.org/10.2343/geochemj.2.0476>
- Liu BJ, Peng SH, Liao YY, Long WL (2018) The causes and impacts of water resources crises in the Pearl River Delta. *J Clean Prod* 177:413–425. <https://doi.org/10.1016/j.jclepro.2017.12.203>
- Lucchese LV, de Oliveira GG, Pedrollo OC (2021) Investigation of the influence of nonoccurrence sampling on landslide susceptibility assessment using Artificial Neural Networks. *CATENA* 198:105067. <https://doi.org/10.1016/j.catena.2020.105067>
- Luoma S, Okkonen J, Korkka-Niemi K (2017) Comparison of the AVI, modified SINTACS and GALDIT vulnerability methods under future climate-change scenarios for a shallow low-lying coastal aquifer in southern Finland. *Hydrogeol J* 25(1):203–222. <https://doi.org/10.1007/s10040-016-1471-2>
- M. L. R., (2017a) Guidelines for the assessment of zones of groundwater overdraft (GB/T 34968–2017). Ministry of Water Resources of the People's Republic of China, Beijing (in Chinese)
- M. L. R., (2017b) Standard for groundwater quality (GB/T 14848–2017). Ministry of Land and Resources of the People's Republic of China, Beijing (in Chinese)
- M. W. R., (2005) Groundwater functional zoning outline. Ministry of Water Resources of the People's Republic of China, Beijing (in Chinese)
- Ma X (2018) Groundwater resources evaluation of the ZhenBeiPu area in Yinchuan of Ningxia. China University of Geosciences, Beijing (in Chinese)
- Machiwal D, Rangi N, Sharma A (2015) Integrated knowledge- and data-driven approaches for groundwater potential zoning using GIS and multi-criteria decision making techniques on hard-rock terrain of Ahar catchment, Rajasthan. *India Environmental Earth Sciences* 73(4):1871–1892. <https://doi.org/10.1007/s12665-014-3544-7>
- Mahrez B, Klebingat S, Houha B, Houria B (2018) GIS-based GALDIT method for vulnerability assessment to seawater intrusion of the Quaternary coastal Collo aquifer (NE-Algeria). *Arab J Geosci* 11(4):71. <https://doi.org/10.1007/s12517-018-3400-2>
- Majidipour F, Bagher SMB, Taheri K, Fathollahi J, Missimer TM (2021) Index-based groundwater sustainability assessment in the socio-economic context: a case study in the Western Iran. *Environ Manage* 67(4):648–666. <https://doi.org/10.1007/s00267-021-01424-7>
- Manca D, Brambilla S (2011) A methodology based on the Analytic Hierarchy Process for the quantitative assessment of emergency preparedness and response in road tunnels. *Transp Policy* 18(5):657–664. <https://doi.org/10.1016/j.tranpol.2010.12.003>
- Mandal U, Sahoo S, Munusamy SB, Dhar A, Panda SN, Kar A, Mishra PK (2016) Delineation of groundwater potential zones of coastal groundwater basin using multi-criteria decision making

- technique. *Water Resour Manage* 30(12):4293–4310. <https://doi.org/10.1007/s11269-016-1421-8>
- Moghaddam HK, Jafari F, Javadi S (2017) Vulnerability evaluation of a coastal aquifer via GALDIT model and comparison with DRAS-TIC index using quality parameters. *Hydrological Sciences Journal-Journal Des Sciences Hydrologiques* 62(1):137–146. <https://doi.org/10.1080/02626667.2015.1080827>
- Mohammady M, Pourghasemi HR, Amiri M (2019) Land subsidence susceptibility assessment using random forest machine learning algorithm. *Environmental Earth Sciences* 78(16):503. <https://doi.org/10.1007/s12665-019-8518-3>
- Mueller TG, Pusuluri NB, Mathias KK, Cornelius PL, Barnhisel RI, Shearer SA (2001) Map quality for ordinary kriging and inverse distance weighted interpolation. *Soil Sci Soc Am J* 68(6):2042–2047. <https://doi.org/10.2136/sssaj2004.2042>
- Munch Z, Conrad J (2007) Remote sensing and GIS based determination of groundwater dependent ecosystems in the Western Cape. *South Africa Hydrogeology Journal* 15(1):19–28. <https://doi.org/10.1007/s10040-006-0125-1>
- Myronidis D, Papageorgiou C, Theophanous S (2016) Landslide susceptibility mapping based on landslide history and analytic hierarchy process (AHP). *Nat Hazards* 81(1):245–263. <https://doi.org/10.1007/s11069-015-2075-1>
- Najafi Z, Pourghasemi HR, Ghanbarian G, Shamsi SRF (2020) Land subsidence susceptibility zonation using remote sensing, GIS, and probability models in a Google Earth Engine platform. *Environmental Earth Sciences* 79(21):491. <https://doi.org/10.1007/s12665-020-09238-2>
- Narimani R, Jun C, Shahzad S, Oh J, Park K (2021) Application of a novel hybrid method for flood susceptibility mapping with satellite images: a case study of Seoul. *Korea Remote Sensing* 13(14):2786. <https://doi.org/10.3390/rs13142786>
- Nouri D, Sabour MR, Ghanbarzadeh Lak M (2018) Industrial solid waste management through the application of multi-criteria decision-making analysis: a case study of Shamsabad industrial complexes. *J Mater Cycles Waste Manage* 20(1):43–58. <https://doi.org/10.1007/s10163-016-0544-6>
- Oh HJ, Syifa M, Lee CW, Lee S (2019) Land subsidence susceptibility mapping using Bayesian, functional, and meta-ensemble machine learning models. *Applied Sciences-Basel* 9(6):1248. <https://doi.org/10.3390/app9061248>
- Ozdemir A (2016) Sinkhole susceptibility mapping using logistic regression in KarapA +/- nar (Konya, Turkey). *Bull Eng Geol Env* 75(2):681–707. <https://doi.org/10.1007/s10064-015-0778-x>
- Pamucar D, Stevic Z, Zavadskas EK (2018) Integration of interval rough AHP and interval rough MABAC methods for evaluating university web pages. *Appl Soft Comput* 67:141–163. <https://doi.org/10.1016/j.asoc.2018.02.057>
- Panahi MR, Mousavi SM, Rahimzadegan M (2017) Delineation of groundwater potential zones using remote sensing, GIS, and AHP technique in Tehran-Karaj plain. *Iran Environmental Earth Sciences* 76(23):792. <https://doi.org/10.1007/s12665-017-7126-3>
- Pandey VP, Shrestha S, Chapagain SK, Kazama F (2011) A framework for measuring groundwater sustainability. *Environ Sci Policy* 14(4):396–407. <https://doi.org/10.1016/j.envsci.2011.03.008>
- Paz MC, Alcalá FJ, Medeiros A, Martínez-Pagan P, Pérez-Cuevas J, Ribeiro L (2020) Integrated MASW and ERT imaging for geological definition of an unconfined alluvial aquifer sustaining a coastal groundwater-dependent ecosystem in Southwest Portugal. *Applied Sciences-Basel* 10(17):5905. <https://doi.org/10.3390/app10175905>
- Peng J, Peng FL (2018) A GIS-based evaluation method of underground space resources for urban spatial planning: part I methodology. *Tunn Undergr Space Technol* 74:82–95. <https://doi.org/10.1016/j.tust.2018.01.002>
- Pires A, Morato J, Peixoto H, Botero V, Zuluaga L, Figueroa A (2017) Sustainability assessment of indicators for integrated water resources management. *Sci Total Environ* 578:139–147. <https://doi.org/10.1016/j.scitotenv.2016.10.217>
- Podvezko V (2009) Application of AHP technique. *J Bus Econ Manag* 10(2):181–189. <https://doi.org/10.3846/1611-1699.2009.10.181-189>
- Pournader M, Ahmadi H, Feiznia S, Karimi H, Peirovan HR (2018) Spatial prediction of soil erosion susceptibility: an evaluation of the maximum entropy model. *Earth Sci Inf* 11(3):389–401. <https://doi.org/10.1007/s12145-018-0338-6>
- Quan HC, Lee BG (2012) GIS-based landslide susceptibility mapping using analytic hierarchy process and artificial neural network in Jeju (Korea). *KSCE J Civ Eng* 16(7):1258–1266. <https://doi.org/10.1007/s12205-012-1242-0>
- Rachid G, Alameddine I, Abou Najm M, Qian S, El-Fadel M (2021) Dynamic Bayesian networks to assess anthropogenic and climatic drivers of saltwater intrusion: a decision support tool toward improved management. *Intergrated Environmental Assessment and Management* 17(1):202–220. <https://doi.org/10.1002/ieam.4355>
- Raghavendra SN, Deka PC (2015) Sustainable development and management of groundwater resources in mining affected areas: a review. *Procedia Earth and Planetary Science* 11:598–604. <https://doi.org/10.1016/j.proeps.2015.06.061>
- Rahmati O, Falah F, Naghibi S, A., Biggs, T., Soltani, M., Deo, R. C., Cerda, A., Mohammadi, F., Bui D. T., (2019) Land subsidence modelling using tree-based machine learning algorithms. *Science of Total Environment* 672:239–252. <https://doi.org/10.1016/j.scitotenv.2019.03.496>
- Recinos N, Kallioras A, Pliakas F, Schuth C (2015) Application of GALDIT index to assess the intrinsic vulnerability to seawater intrusion of coastal granular aquifers. *Environmental Earth Sciences* 73(3):1017–1032. <https://doi.org/10.1007/s12665-014-3452-x>
- Reddy BP, Kelly MP, Thokala P, Walters SJ, Duenas A (2014) Prioritising public health guidance topics in the National Institute for Health and Care Excellence using the Analytic Hierarchy Process. *Public Health* 128(10):896–903. <https://doi.org/10.1016/j.puhe.2014.07.003>
- Roy J, Saha S (2021) Integration of artificial intelligence with meta classifiers for the gully erosion susceptibility assessment in Hinglo river basin. *Eastern India Advances in Space Research* 67(1):316–333. <https://doi.org/10.1016/j.asr.2020.10.013>
- Saaty TL (1980) *The analytic hierarchy process: planning, priority setting, resource allocation*. McGraw-Hill, New York
- Salles LD, Galvao P, Bastos LRB, Pereira RGFD, da Purificacao CGC, Laureano FV (2018) Evaluation of susceptibility for terrain collapse and subsidence in karst areas, municipality of Iraquara, Chapada Diamantina (BA). *Brazil Environmental Earth Sciences* 77(16):593. <https://doi.org/10.1007/s12665-018-7769-8>
- Sallwey J, Valverde JPB, Lopez FV, Junghanns R, Stefan C (2019) Suitability maps for managed aquifer recharge: a review of multi-criteria decision analysis studies. *Environmental Review* 27(2):138–150. <https://doi.org/10.1139/er-2018-0069>
- Sangrat W, Thanapongtharm W, Poolkhet C (2020) Identification of risk areas for foot and mouth disease in Thailand using a geographic information system-based multi-criteria decision analysis. *Prev Vet Med* 185:105183. <https://doi.org/10.1016/j.prevetmed.2020.105183>
- Seenipandi K, Nainarpandian C, Kandathil RK, Sellamuthu S (2019) Seawater intrusion vulnerability in the coastal aquifers of southern India-an appraisal of the GALDIT model, parameters' sensitivity, and hydrochemical indicators. *Environ Sci Pollut Res* 26(10):9755–9784. <https://doi.org/10.1007/s11356-019-04401-0>

- Senouci R, Taibi NE, Teodoro AC, Duarte L, Mansour H, Meddah RY (2021) GIS-Based Expert Knowledge for Landslide Susceptibility Mapping (LSM): Case of Mostaganem Coast District. *West of Algeria Sustainability* 13(2):630. <https://doi.org/10.3390/su13020630>
- Sholagberu AT, Ul Mustafa MR, Yusof KW, Hashim AM, Shah MM, Khan MWA, Isa MH (2019) Multivariate logistic regression model for soil erosion susceptibility assessment under static and dynamic causative factors. *Polish Journal of Environmental Studies* 28(5):3419–3429. <https://doi.org/10.15244/pjoes/91943>
- Shu BR, Bakker MM, Zhang HH, Li YL, Qin W, Carsjens GJ (2017) Modeling urban expansion by using variable weights logistic cellular automata: a case study of Nanjing, China. *Int J Geogr Inf Sci* 31(7):1314–1333. <https://doi.org/10.1080/13658816.2017.1283505>
- Singh AP, Bhakaru P (2021) Development of groundwater sustainability index: a case study of western arid region of Rajasthan. *India Environment Development and Sustainability* 23(2):1844–1868. <https://doi.org/10.1007/s10668-020-00654-9>
- Singh LK, Jha MK, Chowdary VM (2018) Assessing the accuracy of GIS-based Multi-Criteria Decision Analysis approaches for mapping groundwater potential. *Ecol Ind* 91:24–37. <https://doi.org/10.1016/j.ecolind.2018.03.070>
- Slama T, Sebei A (2020) Spatial and temporal analysis of shallow groundwater quality using GIS, Grombalia aquifer, Northern Tunisia. *J Afr Earth Sc* 170:103915. <https://doi.org/10.1016/j.jafrearsci.2020.103915>
- Soyaslan II (2020) Assessment of groundwater vulnerability using modified DRASTIC-Analytical Hierarchy Process model in Bucak Basin. *Turkey Arabian Journal of Geosciences* 13(21):1127. <https://doi.org/10.1007/s12517-020-06101-3>
- Steele K, Carmel Y, Cross J, Wilcox C (2009) Uses and misuses of multicriteria decision analysis (MCDA) in environmental decision making. *Risk Anal* 29(1):26–33. <https://doi.org/10.1111/j.1539-6924.2008.01130.x>
- Sullivan C (2002) Calculating a water poverty index. *World Dev* 30(7):1195–1210. [https://doi.org/10.1016/S0305-750X\(02\)00035-9](https://doi.org/10.1016/S0305-750X(02)00035-9)
- Sun LW, Ma CM, Li YG (2019) Multiple geo-environmental hazards susceptibility assessment: a case study in Luoning County, Henan Province. *China Geomatics Natural Hazards & Risk* 10(1):2009–2029. <https://doi.org/10.1080/19475705.2019.1658648>
- Tafreshi GM, Nakhaei M, Lak R (2020) A GIS-based comparative study of hybrid fuzzy-gene expression programming and hybrid fuzzy-artificial neural network for land subsidence susceptibility modeling. *Stoch Env Res Risk Assess* 34(7):1059–1087. <https://doi.org/10.1007/s00477-020-01810-3>
- Taheri K, Gutierrez F, Mohseni H, Raeisi E, Taheri M (2015) Sinkhole susceptibility mapping using the analytical hierarchy process (AHP) and magnitude-frequency relationships: A case study in Hamadan province. *Iran Geomorphology* 234:64–79. <https://doi.org/10.1016/j.geomorph.2015.01.005>
- Taheri K, Shahabi H, Chapi K, Shirzadi A, Gutierrez F, Khosravi K (2019) Sinkhole susceptibility mapping: a comparison between Bayes-based machine learning algorithms. *Land Degradation Development* 30(7):730–745. <https://doi.org/10.1002/ldr.3255>
- Tangestani MH (2004) Landslide susceptibility mapping using the fuzzy gamma approach in a GIS, Kakan catchment area, southwest Iran. *Aust J Earth Sci* 51(3):439–450. <https://doi.org/10.1111/j.1400-0952.2004.01068.x>
- Trabelsi N, Triki I, Hentati I, Zairi M (2016) Aquifer vulnerability and seawater intrusion risk using GALDIT, GQI(SWI) and GIS: case of a coastal aquifer in Tunisia. *Environmental Earth Sciences* 75(8):669. <https://doi.org/10.1007/s12665-016-5459-y>
- Turk A, Ozkok M (2020) Shipyard location selection based on fuzzy AHP and TOPSIS. *Journal of Intelligent & Fuzzy Systems* 39(3):4557–4576. <https://doi.org/10.3233/JIFS-200522>
- U. S. G. S., (2020) Land subsidence in the United States. United States Geological Survey, Reston
- Unver S, Ergenc I (2021) Safety risk identification and prioritize of forest logging activities using analytic hierarchy process (AHP). *Alex Eng J* 60(1):1591–1599. <https://doi.org/10.1016/j.aej.2020.11.012>
- Vahidnia MH, Alesheikh AA, Alimohammadi A (2009) Hospital site selection using fuzzy AHP and its derivatives. *J Environ Manage* 90(10):3048–3056. <https://doi.org/10.1016/j.jenvman.2009.04.010>
- Vaidya OS, Kumar S (2006) Analytic hierarchy process: an overview of applications. *European Journal of Operational Research* 169(1):1–29. <https://doi.org/10.1016/j.ejor.2004.04.028>
- Veerappan R, Negi A, Siddan A (2017) Landslide susceptibility mapping and comparison using frequency ratio and analytical hierarchy process in part of NH-58, Uttarakhand, India. *Advancing Culture of Living with Landslides. Advances in Landslide Science* 2:1081–1091. https://doi.org/10.1007/978-3-319-53498-5_123
- Vrba J, Lipponen A (2007) Groundwater resources sustainability indicators, IHP-VI, Series on Groundwater NO. 14. U. N. E. S. C. O., I. A. E. A., I. A. H.
- W. C. G. S., (2015) Evaluation report on the resources and environment carrying capacity of the Pearl River Delta. Wuhan Center of Geological Survey, Wuhan (in Chinese)
- Wada CA, Pongkijyorasin S, Burnett KM (2020) Mountain-to-sea ecological-resource management: Forested watersheds, coastal aquifers, and groundwater dependent ecosystems. *Resource and Energy Economics* 59:101146. <https://doi.org/10.1016/j.reseneeco.2019.101146>
- Wang P (1985) Fuzzy set and random set shadow. Beijing Normal University Press, Beijing (in Chinese)
- Wang Y, Jiao JJ (2012) Origin of groundwater salinity and hydro-geochemical processes in the confined Quaternary aquifer of the Pearl River Delta, China. *J Hydrol* 438:112–124. <https://doi.org/10.1016/j.jhydrol.2012.03.008>
- Wang Y, Jiao JJ, Zhang K, Zhou YZ (2016) Enrichment and mechanisms of heavy metal mobility in a coastal quaternary groundwater system of the Pearl River Delta, China. *Sci Total Environ* 545:493–502. <https://doi.org/10.1016/j.scitotenv.2015.12.019>
- Wang JS, Diao MZ, Yue KH (2017) Optimization on pinch point temperature difference of ORC system based on AHP-entropy method. *Energy* 141:97–107. <https://doi.org/10.1016/j.energy.2017.09.052>
- Wang H, Jin YN, Tan X (2020) Study on sustainable development of the transnational power grid interconnection projects under diversified risks based on variable weight theory and Bayesian network. *Math Probl Eng* 2020:5361561. <https://doi.org/10.1155/2020/5361561>
- Wei X, Wu CY (2011) Holocene delta evolution and sequence stratigraphy of the Pearl River Delta in South China. *Science China-Earth Sciences* 54(10):1523–1541. <https://doi.org/10.1007/s11430-011-4238-6>
- Wei AH, Li D, Zhou YH, Deng Q, Yan LD (2021) A novel combination approach for karst collapse susceptibility assessment using the analytic hierarchy process, catastrophe, and entropy model. *Nat Hazards* 105(1):405–430. <https://doi.org/10.1007/s11069-020-04317-w>
- Wu CS, Yang SL, Huang SC, Mu JB (2016) Delta changes in the Pearl River estuary and its response to human activities (1954–2008). *Quatern Int* 392:147–154. <https://doi.org/10.1016/j.quaint.2015.04.009>

- Wu Q, Zhao DK, Wang Y, Shen JJ, Mu WP, Liu HL (2017) Method for assessing coal-floor water-inrush risk based on the variable-weight model and unascertained measure theory. *Hydrogeology Journal* 25(7):2089–2103. <https://doi.org/10.1007/s10040-017-1614-0>
- Wu YB, Jiang XZ, Guan ZD, Luo WQ, Wang YL (2018) AHP-based evaluation of the karst collapse susceptibility in Tailai Basin, Shandong Province. *China Environmental Earth Sciences* 77(12):436. <https://doi.org/10.1007/s12665-018-7609-x>
- Wu XJ, Zhang L, Hu BX, Wang Y, Xu ZY (2020) Isotopic and hydrochemical evidence for the salinity origin in the coastal aquifers of the Pearl River Delta, Guangzhou. *China Journal of Contaminant Hydrology* 235:103732. <https://doi.org/10.1016/j.jconhyd.2020.103732>
- Xu W, Su XS (2019) Challenges and impacts of climate change and human activities on groundwater-dependent ecosystems in arid areas - a case study of the Nalenggele alluvial fan in NW China. *J Hydrol* 573:376–385. <https://doi.org/10.1016/j.jhydrol.2019.03.082>
- Yadegaridehkordi E, Nasir MHN, Noor NFBM, Shuib L, Badie N (2018) Predicting the adoption of cloud-based technology using fuzzy analytic hierarchy process and structural equation modelling approaches. *Appl Soft Comput* 66:77–89. <https://doi.org/10.1016/j.asoc.2017.12.051>
- Yan QY, Zhang MJ, Li W, Qin GY (2020) Risk assessment of new energy vehicle supply chain based on variable weight theory and cloud model: a case study in China. *Sustainability* 12(8):3150. <https://doi.org/10.3390/su12083150>
- Yang J, Tang ZH, Jiao T, Muhammad AM (2017) Combining AHP and genetic algorithms approaches to modify DRASTIC model to assess groundwater vulnerability: a case study from Jiangnan Plain. *China Environmental Earth Sciences* 76(12):426. <https://doi.org/10.1007/s12665-017-6759-6>
- Yaraghi N, Tabesh P, Guan PQ, Zhuang J (2015) Comparison of AHP and Monte Carlo AHP under different levels of uncertainty. *IEEE Trans Eng Manage* 62(1):122–132. <https://doi.org/10.1109/TEM.2014.2360082>
- Yilmaz I (2007) GIS based susceptibility mapping of karst depression in gypsum: a case study from Sivas basin. *Eng Geol* 90(1–2):89–103. <https://doi.org/10.1016/j.enggeo.2006.12.004>
- Yu CS (2002) A GP-AHP method for solving group decision-making fuzzy AHP problems. *Comput Oper Res* 29(14):1969–2001. [https://doi.org/10.1016/S0305-0548\(01\)00068-5](https://doi.org/10.1016/S0305-0548(01)00068-5)
- Zarghami E, Azemati H, Fatourehchi D, Karamloo M (2018) Customizing well-known sustainability assessment tools for Iranian residential buildings using Fuzzy Analytic Hierarchy Process. *Build Environ* 128:107–128. <https://doi.org/10.1016/j.buildenv.2017.11.032>
- Zhang ZH, Li LR (2005) *China resources of China*. Sino Maps Press, Beijing (in Chinese)
- Zhang QQ, Sun JC, Liu JT, Huang GX, Lu C, Zhang YX (2015) Driving mechanism and sources of groundwater nitrate contamination in the rapidly urbanized region of south China. *J Contam Hydrol* 182:221–230. <https://doi.org/10.1016/j.jconhyd.2015.09.009>
- Zhang FG, Huang GX, Hou QX, Liu CY, Zhang Y, Zhang Q (2019a) Groundwater quality in the Pearl River Delta after the rapid expansion of industrialization and urbanization: distributions, main impact indicators, and driving forces. *J Hydrol* 577:124004. <https://doi.org/10.1016/j.jhydrol.2019.124004>
- Zhang J, Wu Q, Mu WP, Du YZ, Tu K (2019b) Integrating the hierarchy-variable-weight model with collaboration-competition theory for assessing coal-floor water-inrush risk. *Environmental Earth Sciences* 78(6):205. <https://doi.org/10.1007/s12665-019-8217-0>
- Zhang M, Huang GX, Liu GX, Zhang Y, Chen ZY, Wang JC (2020) Distributions and origins of nitrate, nitrite, and ammonium in various aquifers in an urbanized coastal area, south China. *J Hydrol* 582:124528. <https://doi.org/10.1016/j.jhydrol.2019.124528>
- Zhang EL, Zhuo JM, Hou L, Fu CH, Guo T (2021) Comprehensive annoyance modeling of forklift sound quality based on rank score comparison and multi-fuzzy analytic hierarchy process. *Appl Acoust* 173:107705. <https://doi.org/10.1016/j.apacoust.2020.107705>
- Zhao W, Gan FP, Meng Y, Zheng ZJ, Liu XM (2018) Application of seismic velocity tomography in investigation of karst collapse hazards, Guangzhou. *China Environmental Earth Sciences* 77(6):258. <https://doi.org/10.1007/s12665-018-7419-1>
- Zheng GZ, Wang YJ, Li C, Wang X (2020) Real-time quantification of human physiological state in high temperature environments based on variable weight theory. *J Therm Biol* 89:102531. <https://doi.org/10.1016/j.jtherbio.2020.102531>
- Zhou YX, Wang LY, Liu JR, Li WP, Zheng YJ (2012) Options of sustainable groundwater development in Beijing Plain, China. *Phys Chem Earth* 47–48:99–113. <https://doi.org/10.1016/j.pce.2011.09.001>

Publisher's Note Springer Nature remains neutral with regard to jurisdictional claims in published maps and institutional affiliations.